Contrib Mineral Petrol (1991) 108:219–240

Contributions to Mineralogy and Petrology

Calculation of CO_2 activities using scapolite equilibria: constraints on the presence and composition of a fluid phase during high grade metamorphism*

David P. Moecher and Eric J. Essene**

University of Michigan, Department of Geological Sciences, Ann Arbor, MI 48109-1063, USA

Received March 16, 1990/Accepted January 9, 1991

Abstract. Thermodynamic and phase equilibrium data for scapolite have been used to calculate CO_2 activities (a_{CO_2}) and to evaluate the presence or absence of a fluid phase in high-grade scapolite bearing meta-anorthosite, granulites, calc-silicates, and mafix xenoliths. The assemblage scapolite–plagioclase–garnet ± quartz may be used to calculate or limit a_{CO_2} by the reaction Meionite + Quartz = Grossular + Anorthite + CO_2. Granulites from four high-grade terranes (Grenville Province, Canada; Sargut Belt, India; Furua Complex, Tanzania; Bergen Arcs, Norway) yield $a_{CO_2} = 0.4$–1, with most > 0.7. For scapolite-bearing granulites from the Furua Complex, in which $a_{CO_2} \geq 0.9$, calculated H_2O activities (a_{H_2O}) based on phlogopite dehydration equilibria are uniformly low (0.1–0.2). The a_{CO_2} calculated for meta-anorthosite from the Grenville Province, Ontario, ranges from 0.2 to 0.8. For Grenville meta-anorthosite also containing epidote, the a_{H_2O} calculated from clinozoisite dehydration ranges from 0.2 to 0.6. Calc-silicates from the Grenville, Sargur, and Furua terranes mostly yield $a_{CO_2} < 0.5$. The presence of calcite and/or wollastonite provides additional evidence for the low a_{CO_2} in calc-silicates. Samples from six xenolith localities (Lashaine, Tanzania; Eifel, W. Germany; Lesotho; Delegate, Gloucester, and Hill 32, Australia) yield a wide range of a_{CO_2} (0.1 to > 1). The calculated fluid activities are consistent with metamorphism (1) in the presence of a mixed CO_2-H_2O fluid phase in which CO_2 is the dominant fluid species but other $C-O-H-S$ species are minor, (2) in the absence of a bulk fluid phase ("fluid-absent metamorphism"), or (3) in the presence of a fluid-bearing melt phase. The results for many granulites and Grenville meta-anorthosite are consistent with the presence of a CO_2-rich, mixed CO_2-H_2O fluid phase. In contrast the relatively restricted and low values of a_{CO_2} for calc-silicates require an H_2O-rich fluid or absence of a fluid phase during metamorphism. The range of values for xenoliths are most consistent with absence of a fluid phase. The primary implication of these results is that a CO_2-rich fluid accounts for the reduced a_{H_2O} in scapolite-bearing granulites. However, scapolite may be stable with a wide range of fluid compositions or in the absence of a fluid phase, and the presence of scapolite is not a priori evidence of a CO_2-rich fluid phase. In addition, close association of scapolite-free mafic granulites with scapolite-bearing granulites having identical mineral compositions in the Furua Complex, and the absence of scapolite from most granulite terranes implies that a CO_2-rich fluid phase is not pervasive on an outcrop scale or common to all granulite terranes.

Introduction

The role of fluids in the petrogenesis of granulite facies rocks has received considerable attention during the last decade. The role of a fluid phase in high-grade metamorphism focuses on two questions: (a) is a bulk fluid phase actually present during high-grade metamorphism (A.B. Thompson 1983); and, (b) is the low H_2O activity (a_{H_2O}) commonly calculated for high-grade rocks necessarily balanced by a high CO_2 activity (a_{CO_2}) in order to maintain $P_{Fluid} = P_{Total}$? In order to address these questions one needs to know the activities of the dominant fluid species (H_2O and CO_2) typically assumed to be present during metamorphism of high-grade rocks. The a_{H_2O} in high-grade rocks is usually calculated from biotite or amphibole dehydration equilibria. In most cases the calculated a_{H_2O} has been shown to be in the range 0.1 to 0.6 (e.g. Wells 1979; Bohlen et al. 1980; Phillips 1980; Percival 1983; Valley et al. 1983; Bhattacharya and Sen 1986; Newton 1986; Hansen et al. 1987; Lamb and Valley 1988). Except in unusual cases (e.g. Valley et al. 1983), application of these equilibria is complicated by large dilutions of the end-member hydrous phase in solid solu-

---

* Contribution No. 474 from the Mineralogical Laboratory, University of Michigan

** Present Address: Department of Earth and Space Sciences, State University of New York, Stony Brook, N.Y. 11794-2100

Offprint requests to: D.P. Moecher

tions, lack of a comprehensive solution model for the mixing properties of biotites or hornblendes, and poor correspondence between the material on which the experimental or thermodynamic data were collected and the natural phase. Although the accuracy of such calculations may be questioned, the general pattern of low a_{H_2O} is consistent with the interpretation that granulites formed at relatively low p_{H_2O}; this has become a tenet of metamorphic petrology (Eskola 1939; Winkler 1979; Turner 1981; Newton 1986).

Three mechanisms resulting in low a_{H_2O} in granulites are usually enumerated (e.g. Lamb and Valley 1985; Newton 1986; Frost and Frost 1987): (1) the presence of another fluid species (e.g. CO_2), but maintaining $P_{Fluid}=P_{Total}$; (2) metamorphism of anhydrous igneous protoliths or rocks having experienced previous high-grade metamorphic events; or (3) the result of formation of a melt phase and/or passage of H_2O-undersaturated melts through a terrane.

The presence of CO_2 as the primary fluid species that results in reduced a_{H_2O} has been inferred mainly from fluid inclusion studies of granulites (Coolen 1982; Hansen et al. 1984; Schreurs 1984; Santosh 1986). However, in some instances the presence of CO_2-rich fluid inclusions has been shown to be inconsistent with peak fluid composition calculated from mineral equilibria (Lamb and Valley 1985; Lamb et al. 1987).

The a_{CO_2} attending high-grade metamorphism is less amenable to direct calculation because CO_3-bearing phases are relatively uncommon in high-grade silicate lithologies compared to hydrous phases. However, scapolite solid solutions (marialite: $Na_4Al_3Si_9O_{24}Cl$ – meionite: $Ca_4Al_6Si_6O_{24}CO_3$ – sulfate meionite: $Ca_4Al_6Si_6O_{24}SO_4$) have been reported in a number of granulites and high-grade gneisses. Scapolite equilibria thus provide a means to calculate a_{CO_2} independently of other fluid constraints from f_{O_2} and the activity of carbon. The purpose of the present study is to apply the scapolite equilibrium

$$\begin{aligned}&\text{Meionite}+\text{Quartz}=\text{Anorthite}+\text{Grossular}+CO_2\\&2\,Ca_4Al_6Si_6O_{24}CO_3+SiO_2=\\&\quad 5\,CaAl_2Si_2O_8+Ca_3Al_2Si_3O_{12}+2\,CO_2 \qquad (1)\end{aligned}$$

for direct calculation of a_{CO_2} in high-grade rocks with the appropriate mineral assemblage. When possible, the presence or absence of a fluid was evaluated by simultaneous calculation of a_{H_2O} based on biotite or epidote dehydration equilibria. The results place additional constraints on the role of a fluid phase in high-grade metamorphism and the relevance of CO_2 in granulite genesis. The results presented here for granulites and xenoliths incorporate modified activity expressions for meionite in scapolite, and supersede those presented in Moecher (1988) and Moecher and Essene (1990a, b).

Scapolite compositional relations

Numerous studies have demonstrated that scapolite from the upper amphibolite facies tends to be more calcic and carbonate-rich relative to sodic and chlorine-rich varieties typical of lower grade settings (e.g. Hietanen 1967; Kwak 1977; Vanko and Bishop 1982; Mora and Valley 1989). Furthermore, scapolite in granulites, deep-crustal xenoliths, and igneous environments is typically sulfate-rich, with $SO_4/(SO_4+CO_3+Cl)=0.25$ to 0.82 (e.g. references in Table 1 and Fig. 1). These observations are consistent with experimental data indicating a relatively high temperature and/or pressure stability for sulfate scapolite solid solutions (Goldsmith and Newton 1977).

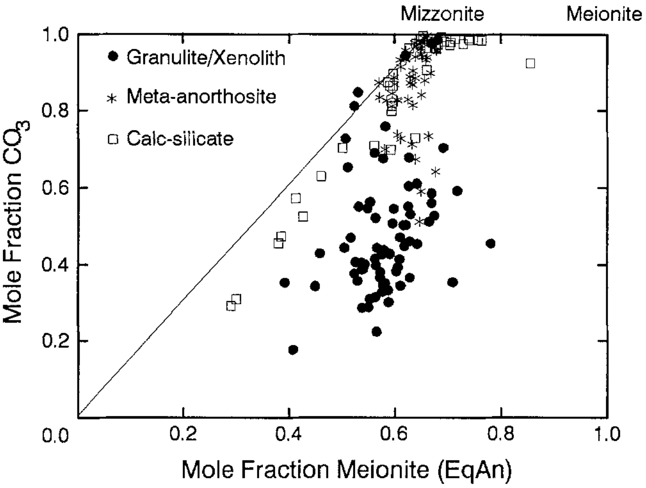

Fig. 1. Compositional range of natural scapolites in terms of EqAn (100(Al-3)/3) and anion site composition X_{CO_3} ($CO_3/[CO_3+SO_4+Cl]$). Samples falling along the trend between mizzonite, ($NaCa_3Al_5Si_7O_{24}CO_3$: EqAn = 67) and EqAn $=X_{CO_3}=0$ are CO_3-Cl solid solutions found in marble, calc-silicate gneisses and skarns, or post-peak metamorphic, brittle, fracture-filling veins. Scapolite in granulites trends from mizzonite toward sulfate-rich, intermediate EqAn compositions. Meta-anorthosite samples falling between CO_3-rich and SO_4-rich mizzonite are from margin and core of Whitestone meta-anorthosite. Sources of data: references in Table 1 and Glassley 1983; Jin et al. 1988; Mezger and Okrusch 1985; Moecher 1988 and unpublished data; Oterdoom and Gunter 1983; Rollinson 1980; Schenk 1984; Stolz 1987 and pers comm; Edwards et al. 1979; Goff et al. 1982; Boivin and Camus 1981

The compositions of scapolite solid solutions encountered in high-grade metamorphic environments define three partly overlapping fields (Fig. 1). Scapolite compositions approaching mizzonite (EqAn = 100(Al-3)/3 = 67, $CO_3/(SO_4+CO_3+Cl)=1$) are common in meta-anorthosite and calc-silicates at upper amphibolite to granulite facies. Sulfate-bearing scapolite in granulites tends to be slightly less calcic than mizzonite but differs from the scapolite described above in the composition of the anion site. More sodic, chlorine-bearing scapolite may occur in high-grade calc-silicates, marbles, or in late, brittle fractures and shears cutting upper amphibolite and granulite facies rocks.

The correspondence of scapolite compositional ranges with metamorphic facies largely reflects the relative P-T stabilities of these compositions. However, it also reflects the activity of fluid components at the time of scapolite formation in each setting, and may be used to constrain fluid activities given appropriate thermodynamic data.

Methods for calculation of CO_2 activities

Thermodynamic data and activity models

Thermodynamic data for meionite and activity-composition (*a*-X) relations for scapolite are necessary in order to calculate a_{CO_2} in high-grade rocks using scapolite equilibria. An internally consistent set of thermodynamic data for meionite, anorthite, grossular, quartz and other calc-silicate phases in the system $CaO-Al_2O_3-SiO_2-CO_2-H_2O$ (CASCH) has been derived based on recently acquired thermodynamic data for scapolite and published experiments in the CASCH system (Moecher and Essene 1990). Thermodynamic calculations were performed with a computer program (EQUILI, Wall and Essene, unpublished; Perkins et al. 1987) that solves the relation

$$\Delta G_{T_2}^{P_2}-\Delta G_{T_1}^{P_1}=\int_{P_1}^{P_2}\Delta V_s\,dP-\int_{T_1}^{T_2}\Delta S_s\,dT+\Delta G(P,T,X)_{H_2O}+\Delta G(P,T,X)_{CO_2}+RT\ln K_2/K_1$$

using available volume, entropy, expansivity and compressibility data.

Anorthite activities were calculated using the ternary feldspar model of Elkins and Grove (1990). Grossular activities for quaternary Gr-Py-Alm-Sp garnets were calculated using the garnet mixing parameters of Anovitz and Essene (1987) as presented in Moecher et al. (1988a).

The activity of meionite in scapolite was calculated following Moecher and Essene (1990c; also see Oterdoom and Gunter 1983) using the experiments of Huckenholz and Seiberl (1989) for the reaction

$$\text{Anorthite}+\text{Calcite}=\text{Meionite}$$

$$3\,CaAl_2Si_2O_8+CaCO_3=Ca_4Al_6Si_6O_{24}CO_3 \qquad (2)$$

to define the standard state free energy of meionite, and the model of Elkins and Grove (1990) to calculate anorthite activities. Moecher and Essene (1990a, b) used the experiments of Goldsmith and Newton (1977) to define the standard state free energy of meionite and the anorthite activity model of Newton et al. (1980a) to calculate anorthite activities. The use of either plagioclase activity model does not significantly affect the conclusions of this study. We assumed a model of complete Al–Si disorder in meionite, consistent with experiments on meionite stability and X-ray diffraction studies. The *a*-X data for natural scapolite–plagioclase–calcite assemblages equilibrated at 600–750° C were fit by least squares to a sub-regular Margules formulation:

$$RT\ln\gamma_{Me}^{Sc}=(1-X_{Me}^{Sc})^2\,[W_G^{Me}+2X_{Me}^{Sc}(W_G^{Ma}-W_G^{Me})]$$

where Me is $Ca_4Al_6Si_6O_{24}CO_3$, Ma is the hypothetical end-member $Na_3Al_3Si_9O_{24}CaCO_3$, and X_{Me}^{Sc} is taken as the equivalent anorthite content (Eq An = [Al-3]/3 for scapolite formula with Si + Al = 12). These relations refer to mixing of 1 mol "$CaAl_2Si_2O_8$" component in pure carbonate scapolite (3 mol $CaAl_2Si_2O_8$ per mol meionite) and are only valid from 600 to 750° C.

The *a*-X relations for $Ca_4Al_6Si_6O_{24}CO_3$ in scapolite are not constrained at temperatures above 750° C, and assumptions must be made for extrapolating them to higher temperatures. A linear dependence of W_G^{Me} and W_G^{Ma} on T results in *a*-X relations that imply negative departures from ideality at $T<750°$ C, and positive deviations from ideality at $T>800°$ C, with the $a_{Me}^{Sc}>1$ at 900° C. These results at $T>750°$ C are solely an artifact of the linear dependence of W_G^{Me} and W_G^{Ma} on T, and are not considered a realistic representation of the behavior of scapolite solid solutions at high T. In order to obtain estimates of meionite activity at $T\geq 800°$ C, we fit the *a*-X relations with a logarithmic dependence of W_G^{Me} and W_G^{Ma} on T (Powell 1974; Ganguly and Saxena 1987), yielding:

$$W_G^{Me}=-\exp[200.5851(1.4247)-29.9065(12.0541)\cdot\ln T]\,(J/mol)$$

$$W_G^{Ma}=-\exp[326.3520(0.8745)-42.2517(11.4056)\cdot\ln T]\,(J/mol)$$

(T in K). Values in parentheses are standard errors for W_H and W_S terms.

Additional assumptions concerning the mixing of CO_3, Cl, and SO_4 in the anion site of scapolite are required in order to apply the *a*-X relations based on pure carbonate scapolite to natural $CO_3-Cl-SO_4$ solid solutions. Based on K_D relations, it appears that the CO_3 and SO_4 groups mix ideally in the anion site in high-grade, Na–Ca scapolite solid solutions (Moecher 1988). Ellis (1978) also presented evidence for ideal mixing between CO_3 and Cl in the anion site for intermediate CO_3-Cl solid solutions. Therefore, the activity of $Ca_4Al_6Si_6O_{24}CO_3$ in a $CO_3-Cl-SO_4$ solid solution was calculated from the mixing relations outlined above, but reduced by the factor $X_{CO_3}=CO_3/(CO_3+SO_4+Cl)$, i.e. $a_{Me}^{Sc}=(\gamma_{Me}^{Sc}\cdot X_{Me}^{Sc})^3\cdot X_{CO_3}$. This differs from that of Moecher and Essene (1990a, b, c), in which the a_{Me}^{Sc} was incorrectly formulated as $[\gamma_{Me}^{Sc}\cdot X_{Me}^{Sc}\cdot X_{CO_3}]^4$. The authors now favor the locally charge balanced mixing model used for scapolite in this paper.

Ideal mixing with a local charge balance (Essene 1989) was assumed for activities of $MgSiO_3$ in orthopyroxene, $Ca_2Al_3Si_3O_{12}(OH)$ in epidote, and $KMg_3AlSi_3O_{10}(OH)_2$ in biotite:

$$a_{CZo}^{Ep}=1-Fe^{3+}\qquad(\text{all }Fe^{3+}\text{ in M1 site})$$

$$a_{En}^{Opx}=X_{Mg}^{Opx}$$

$$a_{Phl}^{Bi}=[X_K\cdot(X_{Mg})^3\cdot(X_{OH})^2].$$

Volatile equilibria

A number of scapolite equilibria are potential CO_2-barometers, particularly for calc-silicate assemblages (e.g. Jones et al. 1983; Moecher and Essene 1990c). The sub-assemblage scapolite (Sc) – plagioclase (Pg) – garnet (Gt) – quartz (Qz) is common to a range of bulk compositions in high-grade rocks, and may be used to calculate a_{CO_2} by Reaction 1. In the absence of quartz, Reaction 1 places an upper limit on a_{CO_2}, and allows constraints on a_{CO_2} to be made in many quartz undersaturated lithologies. Although direct experimental studies of Reaction 1 are lacking, its position was calculated based on experimental and thermodynamic data from other equilibria in the CASCH system.

Moecher and Essene (1990c) demonstrated that the configurational entropy ascribed to Al–Si disorder in meionite has a marked effect on the dP/dT slope of Reactions 1 and 2 (also see Oterdoom and Wenk 1983), and on the degree of departure from ideality of *a*-X relations for meionite. However, if an internally consistent set of thermodynamic data is used to derive the Gibbs free energy of meionite and to model mixing relations of meionite, the same value of a_{CO_2} (within error of the least squares fit to the observed *a*-X relations) is obtained for a sample no matter what value of configurational entropy one assigns to meionite, or which set of experiments one chooses to define the Gibbs free energy of meionite (i.e. Goldsmith and Newton 1977 vs Huckenholz and Seiberl 1989).

In addition, the a_{CO_2} was calculated for calcite (Cc)-bearing meta-anorthosite and calc-silicate gneisses using the reaction

$$\text{Anorthite}+\text{Calcite}+\text{Quartz}=\text{Grossular}+CO_2$$

$$CaAl_2Si_2O_8+2\,CaCO_3+SiO_2=Ca_3Al_2Si_3O_{12}+2\,CO_2. \qquad (3)$$

In rocks that contain the assemgblage Sc-Pg-Gt-Cc-Qz, a_{CO_2} can be calculated from Reaction 1 or 3. The same value of a_{CO_2} should be obtained from each reaction for a given Sc-Pg-Gt-Qz-Cc assemblage because of the dependence of the Gibbs free energy and mixing relations for meionite on thermodynamic data for calcite and anorthite. These assemblages provide a test of the accuracy of a_{CO_2} calculated from Reaction 1. Slight discrepancies in CO_2 derived from the two equilibria may arise from inexact fitting of meionite *a*-X relations.

Values of $\log_{10}K$ for Reaction 1 were calculated using EQUILI and the expression

$$K_1=[(a_{Gr}^{Gt})\cdot(a_{An}^{Pg})^5\cdot(a_{CO_2})^2]/(a_{Me}^{Sc})^2$$

was solved for a_{CO_2} using the appropriate activity models. The a_{CO_2} calculated in the above manner is defined relative to a standard state of pure CO_2 at the pressure and temperature of interest. Alternatively, the fugacity of CO_2 may be calculated using a 1 bar, T standard state.

When possible, a_{H_2O} was calculated using the clinozoisite and phlogopite dehydration equilibria

$$\text{Clinozoisite} + \text{Quartz} = \text{Anorthite} + \text{Grossular} + H_2O$$

$$4Ca_2Al_3Si_3O_{12}(OH) + SiO_2 = 5CaAl_2Si_2O_8 + Ca_3Al_2Si_3O_{12} + 2H_2O \quad (4)$$

$$\text{Phlogopite} + \text{Quartz} = \text{Enstatite} + \text{Sanidine} + H_2O.$$

$$KMg_3AlSi_3O_{10}(OH)_2 + 3SiO_2 = 3MgSiO_3 + KAlSi_3O_8 + H_2O. \quad (5)$$

Reaction 4 was applied to scapolite-bearing Grenville meta-anorthosite with the assemblage epidote(Ep)-Sc-Gt-Pg-Qz. The position and values of $\log_{10}K$ for Reaction 4 were calculated from data in Moecher and Essene (1990c). Reaction 5 was used to calculate a_{H_2O} in granulites from the Furua Granulite Complex, Tanzania. The experimental reversal for Reaction 5 of Bohlen et al. (1983a) (5 kbar, 790° C, $X_{H_2O} = 0.35$) was used as a starting point for the calculation of a_{H_2O}. Entropy and volume data for phlogopite are from Robie and Hemingway (1984) and Hewitt and Wones (1975), respectively. Complete Al–Si disorder was assumed for phlogopite (Clemens et al. 1987). Thermodynamic data for sanidine are from Robie et al. (1978), and data for enstatite and quartz are from sources summarized in Moecher et al. (1988a). The position of the pure H_2O reaction was calculated using the activity coefficient for H_2O at $X_{H_2O} = 0.35$ calculated from the MRK equation of state of Kerrick and Jacobs (1981).

Thermobarometry

For samples of scapolite-bearing calc-silicate gneisses, mafic gneisses, and granulites from the Grenville Province, Ontario, estimates of peak metamorphic pressure and temperature are taken from Anovitz and Essene (1990) and data collected for this study. The samples of meta-anorthosite from the Grenville Province, Ontario, investigated for this study may have re-equilibrated at conditions following the peak of granulite facies metamorphism. For these samples, and samples of scapolite-bearing granulites and xenoliths from other terranes, pressure was primarily calculated using the clinopyroxene (Cpx)-orthopyroxene-plagioclase-garnet-quartz barometers of Moecher et al. (1988a) and Essene (1989). Where appropriate, garnet-Al_2SiO_5-plagioclase-quartz (Lshaine, Tanzania xenoliths) or wollastonite-garnet-plagioclase-quartz barometers (some Grenville calc-silicate rocks) were also applied and yield results consistent with the pyroxene barometers.

Temperature was calculated using the garnet-clinopyroxene Fe–Mg exchange thermometer. Previous applications of garnet-clinopyroxene in high-grade terranes have mainly employed the experimental calibration of Ellis and Green (1979) that in some cases yields results that are consistent with other thermometers and phase equilibrium constraints (e.g. Johnson et al. 1983). However, the garnet-clinopyroxene thermometer has recently been recalibrated experimentally by Pattison and Newton (1989), who observe that their calibration tends to underestimate temperature by as much as 150° C. Pattison and Newton (1989) interpreted this as a tendency for the Fe–Mg exchange between garnet and clinopyroxene to continue with falling temperature after the peak of metamorphism. The following criteria were therefore followed in the calculation of temperature from garnet and clinopyroxene analyses made for this study to minimize possible compositional and retrograde effects (Pattison and Newton 1989):

1) Only electron microprobe analyses of garnet and clinopyroxene cores of the largest grains not in physical contact were used.
2) The highest temperatures were considered best to represent equilibration conditions for a suite of samples. This assumption may be valid for samples taken from regional granulite terranes that equilibrated under broadly similar conditions, but is less likely to hold for xenolith suites that may represent different crustal levels metamorphosed at different times and under variable conditions. In the latter case, if there were significant differences among temperatures obtained for several samples of a xenolith suite, temperatures obtained from each particular sample were used to calculate fluid composition.
3) Estimates of Fe^{3+} calculated from stoichiometry were used in the calculation of K_D.
4) Temperatures were calculated using both calibrations discussed above. Calculations of fluid activity were made at the highest temperature obtained from the two methods (which in most cases was that of Ellis and Green 1979). This convention tends to yield upper limits on a_{CO_2}.

Electron microprobe analyses

Wavelength dispersive electron microprobe analyses were performed on the University of Michigan Cameca CAMEBAX microprobe at an accelerating potential of 15 kV and sample current of 10 nA using natural or synthetic silicate, oxide, and sulfate standards. The Cameca ZAF routine was used to correct raw data. A slightly defocused (2 μm diameter) or rastered beam was used to analyze plagioclase and scapolite to prevent Na migration. Core compositions were generally used in the calculation of a_{CO_2}, although core and rim analyses were commonly collected to evaluate compositional zonation and its effect on a_{CO_2}. Mineral formulae were calculated on the basis of 8 (garnet and epidote), 5 (plagioclase), or 4 (pyroxene) cations, and Fe^{3+} was calculated for garnet and pyroxene on the basis of charge balance and stoichiometry. Scapolite formulae were calculated on the basis of $Si + Al = 12$ (Evans et al. 1969), and $CO_3 + Cl + SO_4 = 1.00$. Representative analyses for meta-anorthosite, calc-silicates, mafic gneisses and granulites from the Grenville Province are listed in the Appendix. Complete analytical data for all Grenville, Bergen, and Sargur samples are presented in Moecher (1988).

Sample descriptions and results

Samples of scapolite-bearing gneisses were collected specifically for this study from upper amphibolite to granulite facies rocks in the Central Gneiss Belt of Ontario, Canada (Moecher 1988). In addition, scapolite-bearing gneisses, granulites, and xenoliths from a number of metamorphic terranes for which chemical analyses of coexisting scapolite, plagioclase, and garnet are available, and which also contain analyses of mineral assemblages appropriate for thermobarometry, have been used to calculate P, T, and a_{CO_2}. In some cases, scapolite-bearing samples were donated by other workers. Values of a_{CO_2} and a_{H_2O} for the following areas are compiled in Tables 1–3, along with the necessary data for their calculation. The calculated a_{CO_2} are also presented in Figs. 2A–D in order better to compare results for each lithology.

Scapolite-bearing gneisses in the Grenville Province

The Central Gneiss Belt in southern Ontario is an upper amphibolite to granulite facies terrane comprised of distinct lithotectonic domains bounded by kilometer-wide zones of high strain and ductile shearing (Davidson 1984,

Table 1. Data and results of calculation of CO_2 activities

A. Meta-anorthosite

Parry Sound, Ontario (Moecher 1988) Sheared southern tail of Whitestone meta-anorthosite. (Sc-Pg-Gt-Hbl ± Qz ± Cpx ± Ep ± Ti ± Ilm ± Bi ± Ap ± Cc)
$P = 10$ kbar, $T = 700°$ C, $K_{P,T} = 0.428$, $\log K_{1,T} = 5.302$

Sample	X_{An}	a_{An}	EqAn	a_{Me}	X_{CO_3}	a_{Gr}	a_{CO_2}	$\log f_{CO_2}$
PS7a	0.49	0.66	0.62	0.45	0.94	0.40	0.73	5.34
PS7b	0.44	0.62	0.58	0.46	0.90	0.43	0.78	5.38
PS7c	0.43	0.61	0.57	0.44	0.98	0.43	0.77	5.37
PS85A-2c	0.57	0.45	0.59	0.42	0.98	0.42	0.64	5.29
PS85A-5*	0.36	0.48	0.57	0.33	0.83	0.32	0.66	5.31
	0.36	0.48	0.61	0.38	0.91	0.32	1.13	5.54
PS085A-8b	0.47	0.60	0.64	0.42	0.88	0.40	0.59	5.26
PS085A-13	0.41	0.54	0.66	0.44	0.99	0.44	0.86	5.42
PS085A-24	0.54	0.67	0.65	0.43	0.84	0.31	0.70	5.33
PS86B1-1	0.38	0.50	0.61	0.38	0.93	0.43	0.67	5.31
PS86B1-10a	0.38	0.50	0.60	0.37	0.89	0.41	0.64	5.29
PS86B1-11	0.50	0.64	0.65	0.43	0.96	0.34	0.76	5.37
PS86B2-1	0.40	0.53	0.57	0.33	0.87	0.42	0.38	5.07
PS86B2-3	0.47	0.60	0.63	0.41	0.87	0.40	0.54	5.22
PS86E-7e	0.45	0.58	0.65	0.43	0.96	0.44	0.68	5.32
PS86E-8	0.48	0.62	0.66	0.44	0.88	0.42	0.61	5.27
PS86E-15	0.51	0.65	0.61	0.37	0.83	0.37	0.36	5.05
PS86E-16a	0.54	0.67	0.66	0.44	0.93	0.36	0.67	5.32
PS86E-24f	0.48	0.62	0.64	0.41	0.81	0.40	0.50	5.18
PS86E-31	0.42	0.56	0.62	0.39	0.96	0.47	0.51	5.20
PS86E-34	0.37	0.50	0.59	0.35	0.83	0.34	0.66	5.31
Eastern margin of main body of Whitestone meta-anorthosite. Same conditions and mineral assemblages as above.								
S85A-3a(c)	0.59	0.72	0.61	0.37	0.83	0.21	0.67	5.31
S85A-3a(r)	0.57	0.70	0.61	0.37	0.84	0.28	0.48	5.16
S85A-3b(c)	0.56	0.69	0.65	0.43	0.98	0.32	0.73	5.35
S85A-3b(r)	0.56	0.69	0.65	0.47	0.98	0.37	0.73	5.35
S85A-3c*	0.50	0.64	0.66	0.48	0.89	0.29	1.09	5.52
S86E-10*	0.52	0.65	0.64	0.42	0.67	0.39	0.38	5.16
	0.52	0.65	0.64	0.41	0.99	0.39	0.54	5.22
S86E-25a	0.52	0.66	0.65	0.44	0.94	0.37	0.63	5.28
S86E-25c(c)	0.46	0.59	0.65	0.43	0.95	0.37	0.83	5.41
S86E-25c(r)	0.46	0.59	0.65	0.43	0.95	0.42	0.68	5.32
S86E-34	0.47	0.61	0.63	0.40	0.83	0.56	0.28	4.94
S86E-36b	0.50	0.63	0.64	0.41	0.90	0.35	0.63	5.29
S86E-41	0.57	0.70	0.66	0.45	1.00	0.27	1.00	5.49
CCM0114	0.62	0.73	0.64	0.56	0.41	0.26	0.45	5.03

1986; van Breemen et al. 1986). Thermobarometric studies have outlined a wide expanse of high pressure rocks within the Central Gneiss Belt, with pressures approaching 11 kbar and peak temperatures in excess of 800° C (Anovitz and Essene 1990). The scapolite-bearing lithologies sampled for this study are primarily in Parry Sound and adjacent domains of the Central Gneiss Belt that attained granulite facies. A detailed description of localities and mineral assemblages for the Grenville samples is presented in Moecher (1988).

The Whitestone Anorthosite. Scapolite is widely developed in the Whitestone Anorthosite (WSA), a 170 km^2 leucocratic gabbroic anorthosite sill (Mason 1969; Nadeau 1983; Thompson 1983; Bright 1987) that was emplaced at approximately 1.35 Ga and underwent granulite facies metamorphism at approximately 1.16 Ga (van Breemen et al. 1986). An upper amphibolite facies metamorphic envelope is developed within the outer 75% of the WSA, characterized by a modal increase in scapolite, hornblende (Hbl), epidote and garnet toward the pluton margins (Mason 1969; D.L. Thompson 1983; Moecher et al. in prep.). The most common mineral assemblage in the envelope is Sc-Pg-Gt-Hbl ± Cpx ± Bi ± ilmenite(Ilm) ± Sp ± apatite(Ap). The envelope is developed around a core of granulite facies meta-anorthosite (Pg-Gt-Cpx-Hbl ± Opx ± Sc ± Qz), where igneous textures are preserved to varying degrees (Mason 1969) or recrystallized to equilibrium granoblastic aggregates. Traces of scapolite are found in some of the Opx-bearing samples from the core of the WSA. Mineral assemblages in the well foliated margin of the WSA exhibit equilibrium granoblastic textures, whereas those between the margin and core may exhibit extensive static replacement of plagioclase, garnet and clinopyroxene by scapolite and hornblende. The WSA is in tectonic contact with a mar-

Table 1. (continued)

B. Calc-silicate gneiss

1. Grenville Province, Ontario (Moecher 1988) (Sc-Pg-Gt ± Qz ± Cc ± Sp ± Cpx ± Wo)
$P = 10$ kbar, $T = 800°$ C, $K_{P,T} = 0.092$, $\log K_{1,T} = 4.864$

Sample	X_{An}	a_{An}	EqAn	a_{Me}	X_{CO_3}	a_{Gr}	a_{CO_2}	$\log f_{CO_2}$
H85A-1b	0.72	0.80	0.69	0.61	0.99	0.61	0.25	4.78
H85A-1d-1	0.68	0.77	0.71	0.64	0.98	0.74	0.23	4.75
H85A-1e(1)	0.44	0.56	0.65	0.57	0.98	0.64	0.45	5.03
H85A-1e(2)	0.51	0.64	0.66	0.58	0.96	0.77	0.30	4.79
M86E-1b	0.25	0.33	0.50	0.40	0.70	0.92	0.26	4.80
M86E-1c-2	0.28	0.36	0.60	0.51	0.87	0.93	0.48	5.06
$P = 10$ kbar, $T = 750°$ C, $K_{P,T} = 0.193$, $\log K_{1,T} = 5.074$								
08e	0.51	0.64	0.66	0.53	0.91	0.82	0.24	4.81
S4d	0.30	0.39	0.59	0.44	0.87	0.89	0.40	5.04
$P = 10$ kbar, $T = 700°$ C, $K_{P,T} = 0.428$, $\log K_{1,T} = 5.302$								
S85A-2a	0.39	0.52	0.62	0.39	0.93	0.85	0.24	4.88
S85A-2b	0.29	0.38	0.60	0.36	0.84	0.87	0.36	5.05
S85A-2d	0.40	0.52	0.60	0.37	0.87	0.86	0.18	4.73
S86E-8c	0.32	0.42	0.60	0.36	0.90	0.65	0.47	5.31
$P = 8$ kbar, $T = 700°$ C, $K_{P,T} = 0.439$, $\log K_{1,T} = 4.922$								
DEB83C-4	0.48	0.62	0.66	0.49	0.98	0.49	0.57	4.86

2. Furua Complex, Tanzania (Coolen 1980). (Sc-Pg-Gt-Cpx ± Ep ± Sp)
$P = 10$ kbar, $T = 800°$ C, $K_{P,T} = 0.092$, $\log K_{1,T} = 4.864$

Sample	X_{An}	a_{An}	EqAn	a_{Me}	X_{CO_3}	a_{Gr}	a_{CO_2}	$\log f_{CO_2}$
ZC-6.2	0.96	0.96	0.78	0.73	0.45	0.73	0.10	4.36
MF-274.2	0.84	0.88	0.69	0.62	0.70	0.88	0.09	4.32

3. Satnur area, Karnataka, India (Devaraju pers. comm. 1987) (Sc-Pg-Gt-Cpx-Sp)
$P = 6$ kbar, $T = 750°$ C, $K_{P,T} = 0.264$, $\mathrm{Log}\, K_{1,T} = 4.352$

Sample	X_{An}	a_{An}	EqAn	a_{Me}	X_{CO_3}	a_{Gr}	a_{CO_2}	$\log f_{CO_2}$
TCD5	0.94	0.95	0.74	0.68	0.99	0.60	0.32	4.15
TCD25	0.93	0.94	0.76	0.71	0.98	0.61	0.38	4.23

C. Granulites, Mafic gneisses

1. Grenville Province, Ontario (Moecher 1988) Mafic gneiss, granulite (Sc-Pg-Gt-Cpx ± Opx ± Hbl ± Bi ± Qz ± Ilm)
$P = 10$ kbar, $T = 800°$ C, $K_{P,T} = 0.092$, $\log K_{1,T} = 4.864$

Sample	X_{An}	a_{An}	EqAn	a_{Me}	X_{CO_3}	a_{Gr}	a_{CO_2}	$\log f_{CO_2}$
80DMA614p	0.51	0.63	0.64	0.56	0.45	0.22	0.72	5.24
85DMP272-2a	0.42	0.53	0.62	0.53	0.45	0.26	0.72	5.24
85DMP174-1a	0.31	0.41	0.56	0.47	0.52	0.24	1.28	5.49
S86E-53a	0.39	0.51	0.60	0.51	0.51	0.33	0.68	5.22
A86B3-3B-3	0.44	0.57	0.61	0.52	0.34	0.16	1.00	5.38
M49	0.42	0.54	0.62	0.53	0.50	0.48	0.31	4.88

ble tectonite breccia along its eastern margin, and primarily Hbl-Pg-Bi-Gt ± Cpx amphibolite on the west.

Although the regional metamorphic temperatures in the vicinity of the WSA for the peak of granulite facies metamorphism are in excess of 800° C, Gt-Cpx temperatures for meta-anorthosite and gneisses in the envelope, and amphibolites along the western margin of the WSA, range from 650 to 750° C (D.L. Thompson 1983; Moecher et al. 1988a). This is consistent with re-equilibration of meta-anorthosite mineral compositions in the margin during cooling from the peak of granulite metamorphism and at a time of differential movement between WSA and enclosing rocks. Geobarometry indicates that pressure was 10 ± 1.5 kbar during the later

Table 1. (continued)

2. Furua Complex, Tanzania. (Coolen 1980, 1982) All granulites (Sc-Pg-Gt-Cpx ± Opx ± Hbl ± Bio ± Qz)
P = 10 kbar, T = 800° C, $K_{P,T} = 0.092$, $\log K_{1,T} = 4.864$

Sample	X_{An}	a_{An}	EqAn	a_{Me}	X_{CO_3}	a_{Gr}	a_{CO_2}	$\log f_{CO_2}$
MF-283.2	0.32	0.42	0.58	0.49	0.35	0.21	1.16	5.45
MF-268.1	0.32	0.42	0.58	0.49	0.44	0.21	1.45	5.54
MF-283.1	0.34	0.44	0.59	0.50	0.33	0.21	1.00	5.38
WE-322.3	0.41	0.52	0.63	0.54	0.46	0.21	1.15	5.44
ZC-8	0.34	0.44	0.56	0.47	0.41	0.21	1.00	5.38
MF-266.3	0.31	0.40	0.55	0.46	0.29	0.20	0.95	5.36
C-247.1	0.33	0.43	0.54	0.44	0.40	0.21	0.91	5.34
C-112	0.35	0.46	0.58	0.48	0.33	0.21	0.81	5.29
C311.1	0.33	0.43	0.55	0.45	0.40	0.22	0.89	5.33
SC-157	0.28	0.36	0.53	0.43	0.36	0.21	1.16	5.45
C-54.1	0.28	0.36	0.57	0.47	0.31	0.21	1.33	5.51
C-52.2	0.30	0.40	0.58	0.49	0.35	0.23	1.09	5.42
SC-156.1	0.35	0.46	0.54	0.44	0.29	0.25	0.43	5.02
C-57	0.29	0.37	0.57	0.47	0.40	0.24	1.31	5.50
C-127	0.34	0.44	0.57	0.47	0.22	0.24	0.47	5.06
C-180.1	0.34	0.45	0.56	0.46	0.37	0.21	0.88	5.33

3. Bergen Arcs, Norway. (Austreim pers. comm. 1987) All granulite facies meta-anorthosite (Sc-Pg-Gt ± Cpx ± Opx ± Hbl ± Ilm/Mt)
P = 11 kbar, T = 900° C, $K_{P,T} = 0.025$, $\log K_{1,T} = 4.642$

Sample	X_{An}	a_{An}	EqAn	a_{Me}	X_{CO_3}	a_{Gr}	a_{CO_2}	$\log f_{CO_2}$
HA10/83	0.50	0.62	0.63	0.59	0.55	0.23	0.54	5.18
HA54/83	0.50	0.61	0.63	0.60	0.37	0.22	0.40	5.05
HA46/85	0.32	0.41	0.53	0.49	0.38	0.21	0.68	5.28
HA53/80	0.31	0.39	0.56	0.52	0.31	0.20	0.76	5.33

4. Sargur Supracrustal Belt, Karnataka, India. Granulites (Sc-Pg-Gt-Opx-Cpx-Hbl-Ilm) from Doddakanya area
P = 9 kbar, T = 800° C, $K_{P,T} = 0.094$, $\log K_{1,T} = 4.693$

Sample	X_{An}	a_{An}	EqAn	a_{Me}	X_{CO_3}	a_{Gr}	a_{CO_2}	$\log f_{CO_2}$
Devaraju pers. comm. (1987)								
TCD33A	0.37	0.48	0.58	0.49	0.43	0.22	0.98	5.37
TCD39	0.38	0.49	0.61	0.52	0.41	0.22	1.04	5.39
Devaraju and Coolen (1982)								
K21	0.39	0.50	0.60	0.51	0.34	0.22	0.78	5.10
Granulite (Sc-Pg-Gt-Opx-Cpx-Hbl-Ilm) from Sargur area (Srikantappa pers. comm. 1987) P = 9 kbar, T = 750° C, $K_{P,T} = 0.194$, $\log K_{1,T} = 4.894$								
285	0.38	0.49	0.57	0.48	0.38	0.21	0.75	5.13

5. Fiordland, New Zealand (Bradshaw 1985, 1989a)
P = 12 kbar, T = 700° C, $K_{P,T} = 0.486$, $\log K_{1,T} = 5.680$

Sample	X_{An}	a_{An}	EqAn	a_{Me}	X_{CO_3}	a_{Gr}	a_{CO_2}	$\log f_{CO_2}$
Feldspathic vein (Pg-Gt-Sc-Qz-Ky-Ru ± Cpx ± Ilm/Mt) cutting orthogneiss.								
112 (core)	0.30	0.43	0.53	0.29	0.81	0.26	0.98	5.83
112 (rim)	0.27	0.39	0.53	0.29	0.85	0.26	1.43	5.99
391 (rim)	0.28	0.40	0.56	0.32	0.69	0.28	1.35	5.97
Feldspathic xenolith (Sc-Pg-Gt-Cpx-Ru) in hornblendite intrusion.								
504	0.29	0.42	0.51	0.27	0.73	0.24	0.85	5.77

Table 1. (continued)

D. Xenoliths

1. Lashaine, Tanzania (Jones et al. 1983) 533 = meta-anorthosite (Sc-Pg-Gt-Ky); all others clinopyroxenites (Sc-Pg-Gt ± Cpx ± Ky ± Ru)
$P = 14$ kbar, $T = 950°$ C, $K_{P,T} = 0.015$, $\log K_{1,T} = 4.904$

Sample	X_{An}	a_{An}	EqAn	a_{Me}	X_{CO_3}	a_{Gr}	a_{CO_2}	$\log f_{CO_2}$
533	0.42	0.52	0.68	0.66	0.99	0.35	0.79	5.69
526	0.29	0.37	0.55	0.53	0.55	0.30	0.67	5.85
528a	0.33	0.41	0.61	0.59	0.47	0.33	0.67	5.82
528b	0.48	0.59	0.61	0.59	0.47	0.33	0.28	5.43
727	0.35	0.44	0.51	0.49	0.65	0.29	0.41	5.56
798a	0.35	0.44	0.62	0.60	0.94	0.28	1.17	5.87
798b	0.35	0.44	0.61	0.58	0.78	0.28	0.89	5.83

528a, b: compositional variation in plagioclase
798a, b: compositional variation in scapolite

2. Eifel, W. Germany (Okrusch et al. 1979) Granulite (Sc-Pg-Gt-Cpx-Hbl-Spinel-Ap)
$P = 10$ kbar, $T = 850°$ C, $K_{P,T} = 0.047$, $\log K_{1,T} = 4.689$

Sample	X_{An}	a_{An}	EqAn	a_{Me}	X_{CO_3}	a_{Gr}	a_{CO_2}	$\log f_{CO_2}$
AS-K-3	0.54	0.65	0.72	0.68	0.59	0.24	0.96	5.34

3. Lesotho, S. Africa (Griffin et al. 1979) Granulites (Sc-Pg-Gt-Cpx ± Hbl ± Opx ± Spinel ± Ky)
P and T as quoted.

Sample	P/T	$K_{P,T}$	X_{An}	a_{An}	EqAn	a_{Me}	X_{CO_3}	a_{Gr}	a_{CO_2}	$\log K_{1,T}$	$\log f_{CO_2}$
K-2	15/750	0.31	0.20	0.25	0.63	0.32	0.60	0.31	6.8	5.97	7.06
PHN2852	14/700	0.62	0.19	0.24	0.57	0.20	0.44	0.27	3.1	6.06	6.65
PHN1670	14/650	1.59	0.23	0.31	0.46	0.09	0.43	0.31	0.14	6.35	5.39
PHN3017	13/750	0.23	0.27	0.34	0.41	0.14	0.18	0.31	0.12	5.61	5.02
L-12A	15/750	0.31	0.19	0.24	0.39	0.13	0.35	0.29	0.72	5.97	6.08
LQ-2	13/750	0.23	0.32	0.42	0.53	0.22	0.55	0.23	1.12	5.61	5.98
LT-2	14/650	1.59	0.27	0.36	0.51	0.16	0.44	0.34	0.16	6.67	5.46

4. Australia

a. Hill 32, Queensland (Rudnick and Taylor 1987) mafic granulite (Sc-Cpx-Gt-Hb-Pg-Ilm-Mt)
$P = 12$ kbar, $T = 950°$ C, $K_{P,T} = 0.014$, $\log K_{1,T} = 4.612$

Sample	X_{An}	a_{An}	EqAn	a_{Me}	X_{CO_3}	a_{Gr}	a_{CO_2}	$\log f_{CO_2}$
85-106	0.45	0.56	0.62	0.60	0.50	0.21	0.59	5.27

b. Gloucester, N.S.W., Australia (Wilkinson 1974) Garnet-plagioclase clinopyroxenite (Sc-Pg-Gt-Cpx-Hbl)
$P = 14$ kbar, $T = 850°$ C, $K_{P,T} = 0.058$, $\log K_{1,T} = 5.313$

R30241	0.38	0.49	0.60	0.54	0.55	0.30	0.79	5.47

c. Delegate, N.S.W. (Lovering and White 1969) Garnet granulite (Sc-Pg-Cpx-Hbl-Sp)
$P = 11$ kbar, $T = 850°$ C, $K_{P,T} = 0.047$, $\log K_{1,T} = 4.831$

R804	0.93	0.94	0.71	0.67	0.35	0.24	0.22	4.61

+ : ($K_{P,T}$) relative to a standard state at the P and T of interest for calculation of a_{CO_2}; $\log K_{1,T}$ relative to a 1 bar and T standard state, based on 1 mole CO_2 for calculation of f_{CO_2}

(c) and (r): core and rim analyses of phases as listed

*: variations in composition among plagioclase, scapolite, or garnet present within a thin section

X: mole fraction; *a*: activity; *f*: fugacity

tectonic displacement (Moecher et al. 1988), similar to peak regional pressures.

Scapolite from the margin of the WSA is dominantly a carbonate-rich mizzonite, with at most 16 mol% Cl or 25 mol% SO_4 (Fig. 1, sample PS7a in Appendix). In contrast, scapolite found in samples from the granulite facies core of the WSA is sulfate-rich with compositions similar to those in granulites (X_{SO_4} up to 50 mol%, Fig. 1, and sample CCM0114, Appendix). There is a systematic decrease in SO_4 and increase in CO_3 content of scapolite from core to margin (Moecher et al. 1988).

The a_{CO_2} calculated for scapolite-bearing samples from the margin of the WSA is variable, with most$=0.7\pm0.2$ (Table 1, Fig. 2A). One sample from the granulite facies core of the WSA (CCM0114) yields $a_{CO_2}=0.45$. Using Reaction 3, calculation of a_{CO_2} for calcite-bearing samples of meta-anorthosite (with or without scapolite) from the southern extension of the WSA yield $a_{CO_2}=0.3$ to 0.6 (Table 2). Two samples with calcite and scapolite (PS86Bl-1, PS86E-31) yield $a_{CO_2}=0.67$ and 0.51 from Reaction 1 compared to 0.48 and 0.45 from Reaction 3. Therefore, the meionite equilibrium tends slightly to overestimate a_{CO_2} relative to that of calcite. In samples where epidote was present along with scapolite, plagioclase, garnet, and quartz, a_{H_2O} calculated using Reaction 4 ranges from 0.1 to 0.5, with most in the range 0.2 to 0.4 (Table 3).

Other rock types. Sulfate/carbonate scapolite occurs in mafic garnet-clinopyroxene gneisses and mafic garnet-granulites from several tectonic domains of the Central Gneiss Belt (Moecher 1988). The mafic gneisses are generally Pg-Cpx-Gt-Sc-Hbl ± Qz assemblages with 5 to 10 modal% hornblende, and which lack biotite. Mafic granulites are distinguished from gneisses by the presence of orthopyroxene. The Grenville gneisses and granulites yield a range of a_{CO_2} from 0.3 to >1 (Fig. 2B).

Carbonate-rich scapolite with up to 20 mol% Cl occurs in low-variance mineral assemblages from high-grade calc-silicates consisting of grossular-rich garnet, calcic plagioclase, diopsidic clinopyroxene, epidote, wollastonite, quartz, sphene, and calcite. In more iron-rich lithologies grossular is more ferrian and the clinopyroxene is hedenbergite. Amphibole and mica are rare or absent from these rocks. Calc-silicate units usually occur as meter scale, discontinuous, conformable lenses interlayered with pelitic or mafic gneisses.

Calc-silicate gneisses from the Grenville Province yield a relatively restricted range of a_{CO_2}. Aside from one sample that yields $a_{CO_2}=0.6$, most of the samples yield $a_{CO_2}<0.5$ (Fig. 2C). Four samples from a two meter-thick calc-silicate lens in the Central Gneiss Belt of Ontario, in which scapolite, plagioclase, and garnet exhibit variable intersample compositions (H85A-1 samples), bracket the range of a_{CO_2} values (0.2 to 0.4) obtained as a result of variable mineral chemistry at constant P and T. For calcite-bearing calc-silicates calculated a_{CO_2} using Reaction 3 are is in the same range as that from Reaction 1 (Table 2, Fig. 2C).

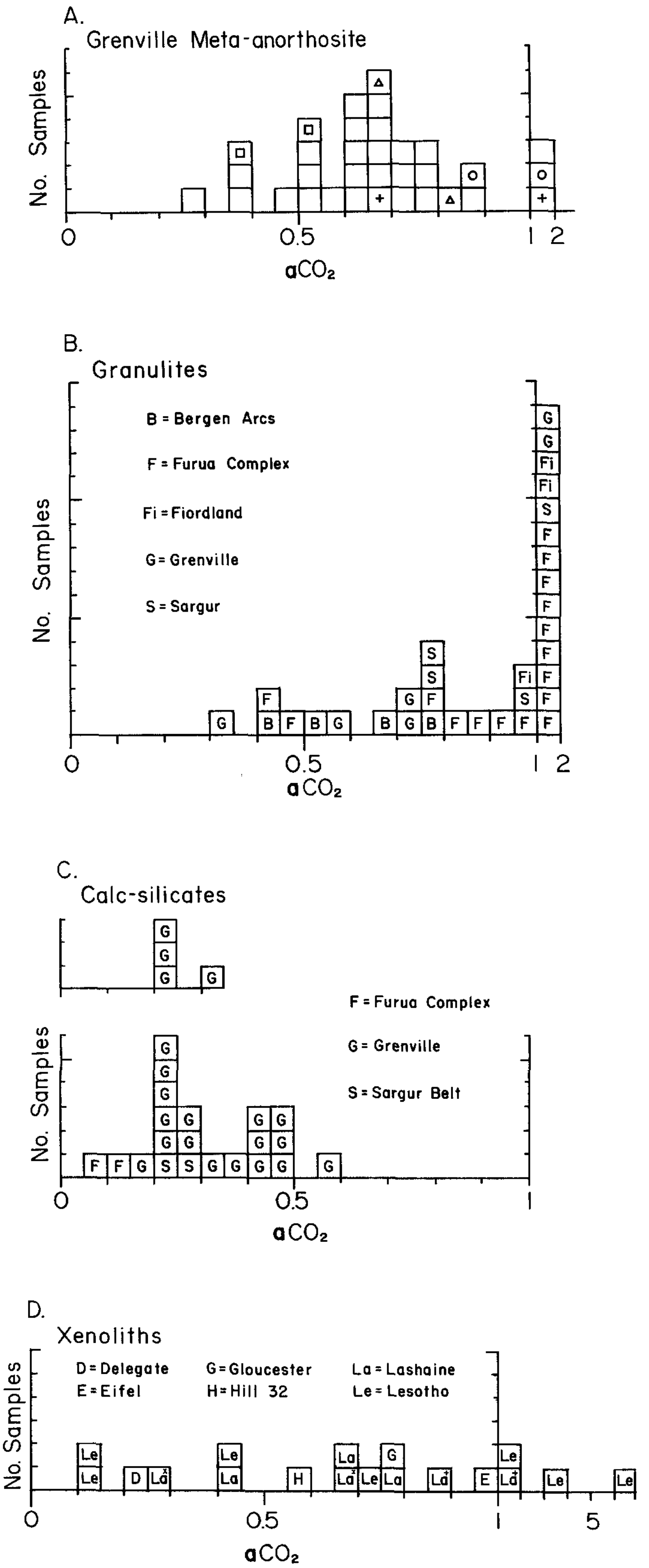

Figs. 2A–D. Histograms summarizing results of calculations of a_{CO_2} as a function of lithology and setting. In **C**, upper values are those calculated from An-Cc-Gr-Qz-CO_2 equilibrium (Reaction 3). Symbols in A and D correspond to a_{CO_2} calculated for intrasample variation in scapolite, plagioclase, or garnet composition (see Table 1), e.g., □ represents valves of a_{co_2} calculated for sample S86E-10 that exhibits two scapolite compositions (see table 1, part A)

Scapolite-bearing gneisses from other granulite terranes

Furua Complex, Tanzania. Coolen (1980) described the petrology and geochemistry of the Furua Complex, a 700 km² granulite terrane in the Pan-African Mozambique Belt of Tanzania. Sulfate-rich scapolite is widely but not pervasively developed in the Furua Complex, occurring in quartz-bearing felsic to mafic two-pyroxene garnet granulites, garnet-clinopyroxene granulites, calc-silicate gneisses, and garnet-clinopyroxene amphibolites.

Estimates of P and T for the Furua Complex obtained with a variety of barometers and thermometers cluster

Table 2. Calculation of CO_2 activities in Grenville calc-silicates and meta-anorthosite with Cc-Pg-Gt-Qz assemblages (Reaction 3)

Sample	P	T °C	$K_{P,T}$	X_{An}	a_{An}	a_{Gr}	a_{CO_2}	log $K_{1,T}$	log f_{CO_2}
Calc-silicates (all with scapolite)									
M86E-1b	10	800	0.10	0.25	0.33	0.92	0.20	4.87	4.68
M86E-1c-2	10	800	0.10	0.28	0.36	0.93	0.21	4.87	4.70
O8e	10	750	0.06	0.51	0.64	0.82	0.34	4.83	4.91
S86E-8c	10	700	0.04	0.32	0.42	0.65	0.24	4.77	4.86

Meta-anorthosite
$P = 10$ kbar, $T = 700°$ C, $K_{P,T} = 0.039$, log $K_{1,T} = 4.77$

Sample	X_{An}	a_{An}	a_{Gr}	a_{CO_2}	log f_{CO_2}
PS7e	0.40	0.53	0.45	0.46	5.15
PS86B1-1+	0.38	0.51	0.43	0.48	5.17
PS86B1-6r	0.15	0.19	0.35	0.40	5.09
PS86B1-6c	0.15	0.19	0.40	0.33	5.01
PS86B1-8	0.15	0.19	0.26	0.61	5.27
PS86B1-9	0.16	0.19	0.35	0.42	5.11
PS86E-31+	0.42	0.56	0.47	0.45	5.14

$K_{P,T}$ relative to a standard state at the P and T of interest for calculation of a_{CO_2}; log $K_{1,T}$ relative to a 1 bar and T standard state, based on 1 mole CO_2 for calculation of f_{CO_2}

+ = samples with scapolite

Table 3. Calculation of H_2O activities using Ep-Gt-Pg-Qz assemblages (Reaction 4) and Bi-Opx-Kfs-Qz assemblages (Reaction 5)

Whitestone meta-anorthosite
$P = 10$ kbar, $T = 700°$ C, $K_{P,T} = 0.038$, log $K_{1,T} = 6.887$

Sample	X_{An}	a_{An}	a_{Gr}	X_{Ps}	a_{CZo}	a_{H_2O}	log f_{H_2O}
PS85A-2c	0.57	0.70	0.42	0.20	0.42	0.30	3.61
PS86B1-11	0.50	0.64	0.34	0.20	0.40	0.47	3.77
PS86E-7e	0.45	0.58	0.44	0.20	0.40	0.41	3.68
PS86E-8	0.48	0.62	0.42	0.22	0.35	0.28	3.54
PS86E-12	0.49	0.63	0.40	0.20	0.40	0.38	3.68
PS86E-15	0.51	0.65	0.37	0.19	0.42	0.44	3.75
PS86E-16a	0.54	0.67	0.36	0.21	0.36	0.31	3.61
PS86E-17	0.55	0.68	0.46	0.21	0.37	0.23	3.48
PS86E-24f	0.48	0.62	0.40	0.19	0.42	0.46	3.75
PS86E-31	0.42	0.56	0.47	0.21	0.36	0.34	3.59
S86E-25a	0.52	0.66	0.37	0.17	0.49	0.58	3.88

Furua Complex granulites
$P = 10$ kbar, $T = 800°$ C, $K_{P,T} = 0.192$, log $K_{1,T} = 3.881$

Sample	X_{En}	X_{Phl}	a_{H_2O}	log f_{H_2O}
MF-283.2	0.55	0.16	0.18	3.68
MF-268.1	0.54	0.14	0.17	3.82
MF-283.1	0.55	0.15	0.17	3.83
ZC-8	0.55	0.12	0.14	3.73
C-180.1	0.60	0.15	0.18	3.73

$K_{P,T}$ and log $K_{1,T}$ as in Table 1

Table 4. Fluid speciation for Furua Complex granulites[a]

Sample	MF-283.2	MF-268.1	MF-283.1	ZC-8	C-180.1
a_{CO_2}	1.16	1.45	1.00	1.00	0.88
log f_{CO_2}	5.45	5.54	5.38	5.38	5.33
p_{CO_2}, kbar	>10	>10	10.0	10.0	8.8
a_{H_2O}	0.18	0.17	0.17	0.14	0.18
log f_{H_2O}	3.86	3.82	3.83	3.73	3.73
p_{H_2O}, kbar	1.1	1.1	1.1	0.9	1.2
P_{Total}[b]	11.1	11.1	11.1	10.9	10.0
log f_{O_2}	−11.1	−11.2	−11.1	−11.1	−10.8
f_{H_2}	0.2	0.2	0.2	0.2	−0.1
log a_C	−2.9	−2.8	−3.0	−3.1	−3.4
log f_{CO}	−1.8	−1.9	−1.7	−1.7	−1.5
log f_{CH_4}	−3.5	−3.4	−3.7	−4.0	−4.6
log f_{S_2}	1.3	1.3	1.3	1.3	1.5
log f_{H_2S}	2.6	2.6	2.6	2.5	2.5
log f_{SO_2}	3.2	3.2	3.3	3.3	3.7
log f_{SO_3}	−2.4	−2.4	−2.3	−2.3	−1.8

[a] Activities (*a*) and fugacities (*f*) of fluid species and carbon in graphite (C) in the C−O−H−S system calculated at 800° C and 10 kbar for Furua Complex granulites that are reported to contain pyrite and magnetite (Coolen 1980). The a_{CO_2} is calculated from equilibrium 1 and a_{H_2O} is calculated from equilibrium 3. p_{CO_2} and p_{H_2O} calculated from a_{CO_2} and a_{H_2O} assuming $P_{Fluid} = P_{Total}$ using MRK equation of state (Kerrick and Jacobs 1981). [b] P_{Total} calculated from sum of p_{CO_2} and p_{H_2O}. For $a_{CO_2} > 1$, $p_{CO_2} = 10$ kbar was assumed as an upper limit

tightly around 10 kbar and 800° C (Coolen 1980; Newton and Perkins 1982; Bohlen et al. 1983b; Moecher et al. 1988a). Kyanite is the stable aluminosilicate in interlayered meta-pelites, restricting temperature to less than 800 ± 50° C at 10 ± 1 kbar. Sixteen samples of granulite gneiss from the Furua Complex yield $a_{CO_2} = 0.4$ to >1 (Fig. 2B). In contrast, two calc-silicate gneisses with sulfate rich scapolite yield $a_{CO_2} = 0.1$.

Several of the scapolite-bearing granulites from the Furua Complex also contain the assemblage Bi-Kfs-Opx-Qz, and were used to evaluate a_{H_2O} by Reaction 5. Biotite was not analyzed for F or Cl in the Furua samples, and therefore the calculated a_{H_2O} are upper limits.

The a_{H_2O} for five samples is uniformly low (0.1 to 0.2, Table 3).

The presence of magnetite and pyrite in the Furua complex samples for which a_{H_2O} was calculated also allow calculation of f_{O_2} and f_{S_2} by the reactions

$$\text{Ferrosilite} + O_2 = \text{Magnetite} + \text{Quartz}$$
$$6FeSiO_3 + O_2 = 2Fe_3O_4 + 6SiO_2 \quad (6)$$

$$\text{Magnetite} + S_2 = \text{Pyrite} + O_2$$
$$Fe_3O_4 + 3S_2 = 3FeS_2 + 2O_2. \quad (7)$$

From f_{O_2}, f_{S_2}, f_{CO_2} and f_{H_2O} the fugacities of fluid species in the C–O–H–S system can be calculated (French 1966). Thermodynamic data for the various fluid species are taken from Robie et al. (1978). At the $f_{O_2}-f_{S_2}$ calculated for these five samples ($\log f_{O_2} = -11$, $\log f_{S_2} = 1$) must other fluid species except for CO_2 and H_2O have low fugacities (Table 4). The species SO_2 and H_2S have the next highest fugacities. Based on fugacity coefficients calculated from the modified Redlich-Kwong (MRK) equation of state of Holloway (1977) and assuming ideal mixing as an approximation, SO_2 and H_2S had calculated partial pressures on the order of 10^2 and 10^1 bars, respectively.

Bergen Arcs, Norway. Sulfate-rich scapolite is reported in granoblastic to coronitic granulite facies meta-anorthosite in the Proterozoic-age Bergen Arcs, Norway (Austrheim and Griffin 1985). Although developed in meta-anorthosite and related rocks, the Bergen samples are grouped here with granulites because their mineral assemblages, geologic setting, and P-T conditions are more similar to granulites and xenoliths than to the Whitestone meta-anorthosite. Based on Gt-Cpx geothermometry and Gt-Opx geobarometry, Austrheim and Griffin (1985) calculated equilibration conditions of 775 to 850° C and 7.8 to 9.4 kbar for meta-anorthosite exhibiting granoblastic textures. Meta-anorthosite exhibiting coronitic textures yielded 875 to 950° C and 8.6 to 12.4 kbar.

Four samples of the Sc-Pg-Gt ± Cpx ± Opx ± Ilm/Mt meta-anorthosite with granoblastic textures were analyzed for this study (Austrheim pers. comm. 1987, data in Moecher 1988). Temperatures and pressures for these samples were calculated to be 875 to 950° C at 12 to 14 kbar; pressure estimates are maxima because quartz is absent from these samples. Calculated a_{CO_2} for the Bergen samples is 0.4 to 0.8 (Fig. 2B).

Sargur Belt, India. Scapolite-bearing mafic granulites occur in the Sargur Belt of southern Karnataka, India (Devaraju and Gowd Reddy 1976; Devaraju and Coolen 1983; Srikantappa et al. 1985). The Sargur Belt consists of elongate (10 to 100 m wide and up to 1 km long) enclaves of pelitic schists, iron formation and calc-silicate, mafic, and ultramafic gneisses within the Peninsular Gneiss of southern India (Viswanatha and Ramakrishnan 1981). The southern part of the belt lies in the transitional area between the upper amphibolite and granulite facies terranes of South India. Kyanite, sillimanite, and kyanite + sillimanite-bearing assemblages are reported from pelitic units within the area (Viswanatha and Ramakrishnan 1981; Janardhan and Srikantappa 1975). Pressure and temperature estimates for this area approach 9 kbar and 800° C for the Doddakanya area (Devaraju and Coolen 1983; Janardhan and Gopalakrishna 1983), and 9 kbar, 750° C for the Sargur area (Srikantappa et al. 1985). Three samples of mafic granulite (Pg-Gt-Sc-Hbl-Opx-Cpx-Ilm) from near Doddakanya and Sargur obtained and analyzed for the present study (Devaraju pers. comm. 1987; Srikantappa pers. comm. 1987) yielded P and T consistent with the previous studies. Values of a_{CO_2} for the Sargur mafic granulites are 0.8 to 1.0 (Fig. 2B).

Carbonate-rich scapolite has been reported in calc-silicate gneisses from the Satnur area of southeastern Karnataka (Devaraju and Sadashivaiah 1964). This area lies within the eastern extent of the transitional terrane, and is intruded locally by the Closepet Granite. Gopalakrishna et al. (1986) calculated P and T of 6 kbar and 750° C from assemblages in meta-pelites and charnockites in the immediate Satnur area. The calc-silicate units occur as meter-sized bodies within mafic granulite and charnockite units. Two samples of Pg-Sc-Gt-Cpx-Ti calc-silicate were analyzed, which yield a_{CO_2} of 0.3–0.4 (Fig. 2C).

Fiordland, New Zealand. Scapolite is reported in garnet-bearing feldspathic veins that cross-cut granulite facies orthogneisses, and also in xenoliths of granulite gneiss entrained within synmetamorphic hornblendite intrusions from the granulite gneiss terrane in southwestern New Zealand (Bradshaw 1989a, b). Veins are interpreted to result from fluid infiltration at or near peak pressure conditions (12 ± 1 kbar at 690 ± 50° C, Bradshaw 1989b). Microprobe data (Bradshaw 1985) indicate that scapolite from two vein assemblages and one xenolith are sulfate-bearing with 20 to 30 mol% SO_4 in the anion site. Rim analyses for two vein-related Fiordland samples yield $a_{CO_2} \geq 1.0$, whereas a xenolith in hornblendite yields $a_{CO_2} = 0.9$ (Fig. 2D).

Mafic xenoliths

Scapolite has been reported in a number of granulite facies mafic xenoliths entrained in kimberlite and alkalic basalt. Most of the scapolite-bearing xenoliths reported in the literature are two-pyroxene granulites (Pg-Cpx-Opx-Sc ± Gt ± Hbl) or garnet clinopyroxenites (Pg-Cpx-Gt-Sc ± kyanite ± rutile). Chemical analyses are presented for the phases of interest in scapolite-bearing mafic xenoliths from Australia, Tanzania, Lesotho, and West Germany. The scapolite present is invariably sulfate rich (e.g. Lovering and White 1969; the most sulfate rich scapolite reported in the literature, $X_{SO_4} = 0.82$ is from Lesotho: Griffin et al. 1979). Pressures calculated for the suite of scapolite-bearing xenoliths are all in excess of 10 kbar, with some approaching 15 kbar (Table 1). They correspond to depths of 30 to 50 km, and most of these xenoliths are likely to have been derived from lowermost continental crust (Kay and Kay 1981; Griffin and O'Reilly 1987; Rudnick and Taylor 1987).

Calculation of precise fluid activities in crustal xenoliths is hampered by equivocal estimates of metamorphic temperature and apparent resetting of equilibria. The requisite assemblage for geothermometry is often present in the scapolite xenoliths. However, a suite of xenoliths may represent more than one metamorphic event, be derived from a range of crustal levels, have had protracted cooling histories in the lower crust, and may have experienced transient re-heating during eruption of the host magma (Kay and Kay 1981). With these caveats in mind, P and T were calculated using the thermobarometric techniques described above.

The lower crustal xenoliths yield the widest range of a_{CO_2} encountered in this study, with most ≤ 1.0 (Fig. 2D). The samples from Lesotho bracket the range of values for all xenoliths (0.1 to $\gg 1$).

Interpretation of calculated a_{CO_2} and a_{H_2O}

The a_{CO_2} for the various settings above is calculated relative to pure CO_2 at the inferred equilibrium P and T. A value of $a_{CO_2} = 1.0$ implies the presence of pure CO_2 fluid during metamorphism. Values of a_{CO_2} less than unity imply metamorphism (1) in the presence of a mixed fluid phase with $P_{Fluid} = P_{Total}$, in which the activity of CO_2 is reduced by other fluid species such as H_2O; (2) in the absence of a free fluid phase; or (3) in the presence of a volatile-bearing melt phase. An a_{CO_2} greater than 1 implies $p_{CO_2} > P_{Total}$, a condition presumed to be structurally unsustainable in metamorphic rocks. In addition, the presence of a pure CO_2 fluid phase is inconsistent with the presence of hydrous phases. Most of the meta-anorthosite and granulite samples contain biotite, hornblende and/or epidote, which require a finite a_{H_2O}. Therefore, a calculated $a_{CO_2} \geq 1$ most likely involves erroneous estimates of a_{CO_2} due to lack of chemical equilibrium among phases, errors in assumed equilibrium T and/or a-X relations for meionite. In certain cases samples that yield calculated $a_{CO_2} > 1$ may provide information regarding retrograde processes in these rocks. For the majority of the analyzed samples, calculated $a_{CO_2} \leq 1.0$ (Fig. 2A–2D), and one of the above cases must hold.

Of the various input parameters needed to calculate a_{CO_2} (metamorphic P-T, microprobe analyses, thermodynamic data, a-X relations), errors in assumed equilibration temperature and a-X relations for meionite in scapolite have the strongest influence on resultant a_{CO_2}. This is primarily due to the temperature dependence of meionite activities below 750° C. In the temperature range 650 to 750° C, a $\pm 50°$ C temperature uncertainty results in a $-50\%/+20\%$ change (relative to calculated value) in a_{CO_2} (this includes the temperature-dependent uncertainties in anorthite and grossular activities). This uncertainty is most serious for a_{CO_2} calculated for rocks inferred to have equilibrated at $T < 750°$ C (e.g. the Whitestone meta-anorthosite, and Fiordland scapolite-bearing veins). The mixing model for meionite discussed above, with the logarithmic dependence of W_G^{Me} on T, yields a much smaller temperature dependence of a_{CO_2} ($<10\%$ relative) at or above 800° C. Thus the temperature dependence of calculated a_{CO_2} is reduced for mafic granulites, granulite facies calc-silicates, and xenoliths.

A second limitation on the absolute precision of the calculated a_{CO_2} arises from the number of moles of meionite, anorthite and grossular in Reaction 1. In the equilibrium constant expression for Reaction 1, the activities of meionite and anorthite components are raised to the sixth, fifth, and third powers (three mol equivalent anorthite component/mol meionite, three mol Ca/mol grossular). Slight variations in a_{Me}^{Sc}, a_{An}^{Pg}, or a_{Gr}^{Gt} (e.g. that might arise from zoning or inter- and intrasample heterogeneity) propagate into relatively large changes in a_{CO_2} (e.g. S85A-3 series, Table 1, all collected from the same outcrop).

Although the a_{CO_2} calculated from meionite equilibria is sensitive to assumed equilibration temperature, we believe the calculated values are reasonably accurate ($\pm 25\%$ relative to calculated value) for several reasons. First, a_{CO_2} calculated from Reaction 3 for Grenville calc-silicates at 800° C and meta-anorthosite at 700° C (Table 2) are in most cases identical to (within error) or less than those from Reaction 1 (Table 1). We believe Reaction 3 places more accurate constraints on a_{CO_2} than Reaction 1 due to better constraints on plagioclase and garnet mixing relations, and more accurate knowledge of the location of Reaction 3 in P-T space. Second, if we assume an equilibration temperature for the Whitestone metaanorthosite 50° C higher than that at which the calculation was performed, most of the calculated a_{CO_2} erroneously exceed 1, and samples of meta-anorthosite for which a_{CO_2} and a_{H_2O} were calculated yield $p_{CO_2} + p_{H_2O} \gg P_{Total}$ (Reaction 4 has a $-50/+100\%$ uncertainty for a temperature uncertainty of $\pm 50°$ C). Third, the calculations are based on an internally consistent set of thermodynamic data that fit available experimental constraints in the CASCH system. This tends to minimize errors resulting from assumed molar free energies, entropies, volumes, etc. If activity models, thermodynamic data, or temperature estimates were greatly in error, we would expect to see more geologically unreasonable values of a_{CO_2} or a_{H_2O}.

The calculation of a_{CO_2} is probably more accurate for the meta-anorthosite and calc-silicate than for granulite and xenolith samples for two reasons. First, the a-X relations for meionite were derived for the temperature range in which the Whitestone meta-anorthosite is inferred to have equilibrated. The a-X relations are best constrained at 600 to 750° C, and assumptions for extrapolation to higher T are not necessary. Second, scapolites in meta-anorthosite and calc-silicates involve limited substitution of SO_4 or Cl in the anion site. This requires no assmptions concerning the extent of nonideality for mixing of CO_3 and SO_4.

Calculation of a_{CO_2} alone does not permit calculation of partial pressures of CO_2 in a real fluid solution, or evaluation of the presence or absence of a fluid phase at the time of peak metamorphism. However, assuming a fluid phase is present, a_{CO_2} may be used to determine X_{CO_2} and X_{H_2O} from the MRK equation of state (Kerrick

Table 5. Fluid speciation for Whitestone meta-anorthosite[a]

Sample	a_{CO_2}	f_{CO_2}	p_{CO_2}	a_{H_2O}	f_{H_2O}	p_{H_2O}	f_{CH_4}	f_{H_2}	f_{O_2}	f_{CO}
PS85A-2c	0.43	5.12	3.4	0.30	3.63	1.8	2.2	1.4	−16.4	2.8
PS86B1-11	0.82	5.40	8.1	0.47	3.83	3.2	2.4	1.4	−16.1	2.8
PS86E-7e	0.74	5.35	7.7	0.41	3.77	2.7	2.3	1.4	−16.2	2.8
PS86E-8	0.67	5.31	6.3	0.28	3.61	1.7	2.0	1.2	−16.2	2.8
PS86E-15	0.34	5.02	2.0	0.44	3.80	3.0	2.7	1.6	−16.5	2.7
PS86E-16a	0.75	5.36	7.3	0.31	3.65	1.9	2.0	1.3	−16.2	2.8
PS86E-24f	0.52	5.20	4.3	0.46	3.82	3.1	2.5	1.6	−16.3	2.7
PS86E-31	0.51	5.19	4.2	0.34	3.68	2.1	2.3	1.3	−16.3	2.7
S86E-25a	0.69	5.26	6.6	0.58	3.92	4.2	2.7	1.6	−16.3	2.8

[a] Activities (*a*) and partial pressures (*p*) (kbar) of CO_2 and H_2O, and fugacities (*f*, $\log_{10}$) of CH_4, H_2, O_2, and CO assuming activity of C in graphite = 1 for Whitestone Anorthosite at 700° C and 10 kbar. Pressures in kbar. p_{CO_2} calculated from a_{CO_2} assuming $p_{CO_2} + p_{H_2O} = P_{Total}$ using MRK equation of state of Kerrick and Jacobs (1981); likewise for p_{H_2O}

and Jacobs 1981) for H_2O-CO_2 mixtures. The X_{CO_2} or X_{H_2O} may then be compared with values of a_{H_2O} typically calculated for high-grade rocks assuming the presence of a fluid phase. For example, at 800° C and 10 kbar, $a_{H_2O} = 0.1$ to 0.3 corresponds to an H_2O-CO_2 fluid with $X_{H_2O} = 0.06$ to 0.20, which requires a_{CO_2} of 0.94 to 0.80.

Whitestone meta-anorthosite

The scapolite-bearing WSA yields variable a_{CO_2}, with most of the values in excess of 0.5. Because these scapolite assemblages are developed in meta-anorthosite that last equilibrated at $T \leq 750°$ C, it is unlikely that partial melting was an important control of fluid activities. Therefore the last equilibration occurred in the presence of a mixed C−O−H−S fluid phase or in the absence of a fluid phase. Calculation of a_{CO_2} and a_{H_2O} for nine samples places constraints on the nature of the fluid phase in the WSA (Table 5). At 700° C and 10 kbar, metamorphism in the presence of a CO_2-rich fluid phase is indicated for five of the samples which yield $p_{H_2O} + p_{CO_2}$ within 1.5 kbar of P_{Total} (Fig. 3). The other samples yield $p_{H_2O} + p_{CO_2} < P_{Total}$ and are consistent with fluid-absent metamorphism.

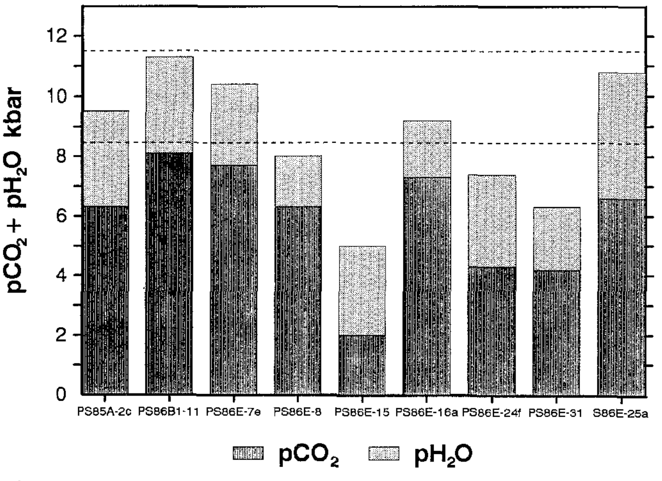

Fig. 3. Histogram of partial pressures of CO_2 and H_2O for Whitestone meta-anorthosite (data summarized in Table 5). *Dashed line* is $\pm 1\sigma$ for lithostatic pressure calculated from mineral equilibria

From the calculated f_{CO_2} and f_{H_2O}, and assuming fluid speciation may be represented by the C−O−H system, limits on f_{O_2}, f_{CH_4}, f_{CO}, and f_{H_2} may be obtained for the scapolite + epidote-bearing meta-anorthosite by assuming a limit on the activity of carbon in graphite of 1 at 700° C and 10 kbar (Table 5). The f_{O_2} is within 0.3 log units of FMQ (−16.5), $\log f_{H_2}$ varies between 1.2 and 1.6, $\log f_{CO}$ is 2.7 to 2.8, and $\log f_{CH_4}$ varies from 2.0 to 2.7. These fugacities correspond to partial pressures of 1–20 bars, based on fugacity coefficients for pure CH_4, CO, and H_2 calculated from the MRK equation of state of Holloway (1977) and assuming ideal mixing. As graphite is absent from these samples, f_{O_2} is a lower limit and f_{CH_4}, f_{CO}, and f_{H_2} are upper limits. The low values for f_{CH_4}, f_{CO}, and f_{H_2} indicate that CO_2 and H_2O would have been the dominant fluid species, and that in samples where $p_{H_2O} + p_{CO_2} \ll P_{Total}$, other C−O−H fluid species do not account for the difference.

A number of meta-anorthosite samples (e.g. PS7 series) yielded calculated CO_2 activities >0.8 (equivalent to X_{CO_2} of 0.8). These samples do not contain epidote, but are hornblende- or biotite-bearing. With their high a_{CO_2} it is possible that these samples also equilibrated in the presence of a mixed CO_2-H_2O fluid phase.

Two samples of meta-anorthosite located between the core and margin of the WSA yield calculated $a_{CO_2} \geq 1$. In S86E-41 ($a_{CO_2} = 1.3$), pure carbonate-scapolite and hornblende, both with ragged grain boundaries, extensively replace plagioclase, clinopyroxene, and garnet, and textural evidence for late infiltration of a mixed $H_2O + CO_2$ fluid is apparent. Garnet in this sample is depleted in grossular component relative to garnet for other meta-anorthosite samples exhibiting equilibrium textural relations with scapolite and plagioclase, and for which calculated $a_{CO_2} < 1.0$ (Table 1). Although erroneous, the high a_{CO_2} for S86E-41 is interpreted to record the effects of retrogression of granulite facies assemblages, in which scapolite is not in equilibrium with garnet or plagioclase at the temperature inferred for other samples of meta-anorthosite. Other samples that yield high a_{CO_2} may exhibit resorbed garnet, or two or more compositional modes and textures of scapolite, plagioclase, or garnet. These are interpreted to result from lack of complete attainment of equilibrium among the phases involved in volatile equilibria.

The development of scapolite and epidote implies that fluid/rock interaction occurred at some point in the metamorphic and tectonic history of the WSA. Stable isotope data for carbon and oxygen for the WSA indicate that the CO_2 necessary to form scapolite was probably derived from marble breccia that is in contact with the main body of the WSA along its eastern margin (Moecher et al. 1988b). However, the results of fluid calculations are not always consistent with metamorphism and shearing in the presence of a fluid phase. In addition, the entire margin of the WSA is not presently in contact with marble (although scapolite-, epidote- and hornblende-bearing assemblages are developed around the entire body) precluding identification of an obvious fluid source for all scapolite-bearing samples. A possible explanation for the rocks that yield low a_{CO_2} or $p_{CO_2} + p_{H_2O} \ll P_{Total}$, is that scapolite and epidote developed during fluid infiltration but before the process of ductile shearing along the margin of the WSA. The well foliated rocks at the margin of the WSA that yield low a_{CO_2} and a_{H_2O} represent the highly sheared and recrystallized equivalents of scapolite-bearing assemblages in the envelope that exhibit retrograde textures and high a_{CO_2}. This recrystallization may have aided in complete reaction of infiltrated CO_2, equilibration of scapolite-plagioclase-garnet-quartz-epidote compositions, and buffering of fluid activities to lower values. Finally, the fluid phase inferred to have reacted with meta-anorthosite may not be well represented by the C–O–H system. The presence of up to 10 to 20 mol percent Cl and/or SO_4 in the anion site in some scapolite may indicate the fluid phase was not a binary CO_2-H_2O fluid. Local enrichments in either a Cl or S component would reduce the carbonate content of scapolite, leading to reduced calculated activities of CO_2.

Granulites

Granulites yield a range of a_{CO_2} with most >0.5. Although scapolites in granulite facies gneisses are slightly less calcic and significantly more sulfate-rich than scapolites from meta-anorthosite and calc-silicates (Fig. 1), plagioclase and garnet in granulite assemblages are characteristically less calcic than those in meta-anorthosite and calc-silicate. The reduced anorthite and grossular activities account for the moderate to high calculated a_{CO_2} in many granulites and xenoliths.

Many of the granulite samples yield $a_{CO_2} \geq 1$. Although most of the values are only slightly greater than 1, these values are clearly erroneous for reasons discussed previously, and at best we can conclude that a_{CO_2} was relatively high compared to calc-silicates and meta-anorthosite. Grenville sample 85DMP174-1a yields one of the highest values for granulites (1.3) that correlates with textural evidence of retrogression (late uralitic alteration of clinopyroxene, resorption of garnet, and late veins of carbonate). However, for many of the granulites that yield high a_{CO_2} there is no textural evidence of disequilibrium cited, and no apparent reason why the calculated a_{CO_2} exceeds one. It is possible that the high calculated a_{CO_2} result from accumulated errors in activity models, temperature and thermodynamic data.

One may ask if the range of a_{CO_2} calculated for terranes such as the Furua Complex is real or merely an artifact of the assumptions of meionite activity models. Assuming ideal mixing of meionite in scapolite (a^{Sc}_{Me} = Eq An content), the calculated range in a_{CO_2} for the Furua samples is not diminished (assuming the same equilibration P and T for these samples). The range of values results from the sensitivity of a_{CO_2} as calculated from Reaction 1 to measurable differences in the mole fractions of meionite, carbonate, anorthite, and grossular. Although the absolute values of a_{CO_2} obtained for a given terrane may be questioned, the relative differences must be real if equilibrium was attained among the appropriate phases.

The a_{H_2O} in five Furua granulites calculated from Reaction 5 is invariably low (0.1–0.2; Table 3). Assuming a fluid phase was present at the peak of metamorphism, the low a_{H_2O} require correspondingly high X_{CO_2}. Although some of the samples yield $a_{CO_2} > 1$, if we assume $a_{CO_2} = 1$ as an upper limit, all five samples yield $p_{CO_2} + p_{H_2O} = P_{Total}$ (Table 4, Fig. 4), and indicate equilibration in the presence of a CO_2-rich fluid phase.

Calculation of fluid speciation for the Furua granulites indicates that the activities/fugacities of other potential fluid species in the C–O–H–S system are generally low at the f_{O_2} and f_{S_2} recorded by mineral equilibria in these samples (Table 4). Although $\log f_{SO_2}$ is nearly as great as that for H_2O, the fugacity coefficient of SO_2 is much larger than that for H_2O (calculated for the pure gas from the MRK equation of state of Holloway 1977), yielding partial pressures on the order of 10–100 bars (assuming ideal mixing). Similar calculations for H_2S indicate partial pressures on the order of 10 bars. The fluid phase that equilibrated with these samples was

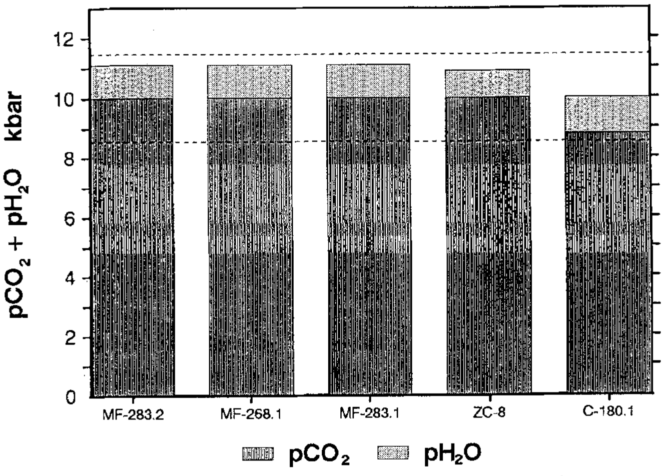

Fig. 4. Histogram of partial pressures of CO_2 and H_2O for Furua Complex granulites (data summarized in Table 4). *Dashed line* is $\pm 1\sigma$ for lithostatic pressure calculated from mineral equilibria. p_{CO_2} is upper possible limit for all samples except C-180.1

dominantly a mixture of CO_2 and H_2O, with minor amounts of SO_2 and H_2S.

The ratio X_{CO_3}/X_{SO_4} is 0.5 to 0.8 in scapolite for the five samples for which $C-O-H-S$ speciation was calculated. In contrast the ratio X_{CO_2}/X_{SO_2} in the fuid phase is approximately 90. At the P, T, and f_{O_2} for the Furua Complex this indicates that CO_2 is preferentially partitioned into the fluid phase relative to scapolite, and SO_2 is preferentially partitioned into scapolite.

Compositional data are not available for calculating a_{H_2O} in the remaining samples from the Furua Complex and other granulite terranes. However, as most granulites yield low a_{H_2O}, if a fluid phase was present during the final equilibration of these rocks it was CO_2-rich and consisted of several fluid species in order for $P_{Fluid} = P_{Total}$. A binary CO_2-H_2O fluid phase with $a_{H_2O} = 0.10$ to 0.30 corresponds to $X_{CO_2} = 0.94$ to 0.70 and $a_{CO_2} = 0.94$ to 0.72. Many of the granulites from this study are consistent with these constraints and with equilibration in the presence of a mixed CO_2-H_2O fluid. In contrast several samples exhibit relatively low a_{CO_2} and, assuming low a_{H_2O}, are more consistent with equilibration in the absence of a bulk fluid phase or in the presence of a melt phase.

Coolen (1980, 1982) documented high-density carbonic fluid inclusions in quartz, plagioclase, and garnet in samples of pelitic and mafic gneiss from the Furua Complex, including two investigated for this study. The calculated fluid composition for mafic granulites MF-268.1 and C-180.1 are consistent with the presence of a CO_2-rich bulk fluid phase with X_{CO_2} of approximately 0.9. A fluid with this composition corresponds to 95 vol% CO_2. The pressure determined by Coolen from the fluid inclusion isochores and inferred metamorphic temperature for these samples was 1–3 kbar lower than that calculated from mineral equilibria. This discrepancy was interpreted to be due to the presence of H_2O in the inclusion (although gas chromatographic analysis of CO_2 liberated by crushing indicated only 1% of other gases). However, the H_2O content required to produce a mixed H_2O-CO_2 fluid with a bulk density that satisfies the requirement of formation at 10 kbar and 800° C (peak P-T) and a CO_2 density of 1.1 g/cm^3 (the average CO_2 density measured by Coolen for inclusions in quartz, plagioclase, and garnet) would be approximately 35 mol% (or about 20 volume %; Brown and Lamb 1989). Although significant amounts of H_2O may be present in small fluid inclusions and not detected optically, it is unlikely that 35 mol% would escape detection either as a separate fluid phase or through the formation of clathrates. The fact that the isochores are not consistent with peak P-T conditions implies formation after the peak of granulite facies metamorphism or post-entrapment alteration of the inclusions, e.g. by leakage of H_2O or an increase in inclusion volumes. In any case, the composition and densities of the fluids in the inclusions are not, in detail, consistent with peak metamorphic P-T-X conditions as inferred from mineral equilibria.

The presence of veins and garnet reaction zones cutting granulite facies orthogneisses in the Fiordland granulite terrane is compelling evidence for channelized fluid infiltration. Bradshaw (1989a) inferred that the first fluids to form the veins were H_2O-rich, as indicated by the formation of hornblende from pyroxene in the orthogneiss host adjacent to veins. The fluid composition was then inferred to become more CO_2-rich, as indicated by the dehydration of hornblende to form garnet, clinopyroxene, quartz, rutile, etc. The presence of scapolite and of CO_2-rich fluid inclusions in quartz, garnet, and plagioclase was taken as evidence for the fluid having been CO_2-rich. However, fluid inclusion isochores are more than 4 kbar below pressure calculated from mineral equilibria, and melting temperatures for inclusions are 1 to 6° C below those for pure CO_2, indicating a component other than CO_2 in the inclusion fluid and/or modification of inclusions following entrapment. Although erroneously high, the a_{CO_2} calculated for this study are consistent with equilibration in the presence of a relatively CO_2-rich fluid phase. Bradshaw (1989a) notes that some scapolite exhibits textural evidence of direct replacement of plagioclase, and it is possible that scapolite did not equilibrate with plagioclase and garnet at or near the inferred peak P-T, thus yielding excessively high a_{CO_2}.

Calc-silicates

Aside from two samples that yield $a_{CO_2} > 0.6$, most of the calc-silicates yield values < 0.5, which are distinct from the other types of rocks investigated. Assuming that melting of calc-silicates is not likely to occur at 700–800° C in a CO_2-H_2O fluid of intermediate X_{CO_2}, the fluid phase was either a mixed $C-O-H-S$ fluid, or metamorphism occurred in the absence of a bulk fluid phase. Epidote is absent from all but one of the calc-silicates examined, precluding the calculation of a_{H_2O} and evaluation of fluid speciation. The low values of a_{CO_2} obtained for some of the calc-silicates indicate, in the presence of calcic plagioclase and grossular-rich garnet, that calcic, carbonate-rich scapolite need not indicate high a_{CO_2} and the presence of a CO_2-rich fluid. Ths conclusion is also supported by calculation of a_{CO_2} using Reaction 3 ($a_{CO_2} = 0.2$, Table 2), and the presence of wollastonite-calcite-quartz in some Grenville calc-silicates which also yield $a_{CO_2} = 0.2$ (M86E-1 samples).

Xenoliths

The xenoliths included in the present study are high-pressure mafic granulites with mineral assemblages and mineral compositions similar to those of granulites from exposed regional terranes. It is not surprising therefore that xenoliths overlap the range of a_{CO_2} for granulites, and conclusions similar to those for granulites hold regarding the role of a fluid phase in the equilibration of xenolith mineral assemblages. In the absence of constraints on a_{H_2O}, f_{O_2}, and f_{S_2}, high a_{CO_2} values are consistent with equilibration in the presence of a mixed $C-O-H-S$ fluid phase, and low a_{CO_2} are consistent with fluid-absent equilibration or the presence of a melt phase.

The suite of xenoliths from Lesotho illustrates the problem of trying to obtain precise estimates of equilibration temperature. The samples exhibit well equilibrated granoblastic textures with no evidence of partial melting (interstitial glass) of any of the phases (Griffin et al. 1979). Some exsolution of garnet, corundum, and spinel from clinopyroxene and plagioclase is noted, but no hydrous retrogression is apparent. Temperatures for six of the samples used here range from 600 to 770° C, and pressures are 12 to 15 kbar. Griffin et al. (1979) report a range in temperature of nearly 200° C for the entire suite of Lesotho granulite xenoliths, and Carswell and Griffin (1981) note a 150° C range for a subset of fourteen samples. It is not known whether these temperatures reflect differential resetting upon cooling, or variation in P-T conditions among various metamorphic episodes and levels in the crust. It is probable that the lower temperatures (600 and 650° C) represent resetting during protracted cooling in the deep crust because they are generally too low for granulite facies metamorphism.

The Lesotho xenoliths yield the widest range of a_{CO_2} for any of the suites examined in this study, with a_{CO_2} that encompasses the values for xenoliths and granulites. The range is a result of two samples, PHN3017 and K-2 which have the lowest and highest X_{CO_3} for the Lesotho suite, and which yield the lowest and highest a_{CO_2} for xenoliths. Temperature variation accounts for some of the differences in calculated a_{CO_2}. For example, calculation of a_{CO_2} for all the samples at 800° C, a more realistic temperature for the granulite facies, yields the same range of a_{CO_2}, but with all samples except PHN3017 yielding $a_{CO_2} > 0.8$. The assumptions for such a calculation are (1) that the samples originally equilibrated at temperatures more representative of the granulite facies; (2) Fe–Mg exchange equilibria between pyroxene and garnet reset independently of the CaAl–NaSi equilibria between plagioclase and scapolite. The range in a_{CO_2} for the Lesotho samples is also due in part to the wide range in composition of relevant phases. Scapolite ranges over 24 mol% Eq An and 42 mol% SO_4, plagioclase over 14 mol% An, and garnet 11 mol% X_{Gr}^{Gt}. This compares with 10 mol% Eq An, 24 mol% X_{SO_4}, 13 mol% An, and 4% X_{Gr}^{Gt} for the Furua granulite samples. The range in composition of the Lesotho samples may reflect sampling of various deep crustal levels.

A more limited range of Gt-Cpx temperatures and a_{CO_2} is obtained for the Lashaine samples, the latter being similar to those for granulites. One sample from Lashaine that yields $a_{CO_2} > 1$ (798) exhibits grain to grain chemical variation in scapolite, with calculated $a_{CO_2} > 1$ for the more CO_3-rich scapolite. As with the Whitestone meta-anorthosite, resetting or lack of complete equilibration of phases on a thin section scale is implied by variable mineral chemistry.

Discussion

Implications for granulite facies metamorphism

The results of this study lend additional support to the conclusion that, when present, the fluid phase in granulite facies lithologies is relatively poor in H_2O. More importantly, these data demonstrate that in some granulites with high calculated a_{CO_2}, lowering of a_{H_2O} is likely to result from the presence of CO_2, as opposed to the complete absence of a bulk fluid phase or due to the presence of a melt phase. In other cases, where granulites yield low a_{CO_2} and are inferred to have equilibrated under low a_{H_2O}, the latter two processes must have contributed to attaining the anhydrous conditions.

Although the calculation of a_{CO_2} from scapolite equilibria provides constraints on the presence and composition of the fluid phase attending final equilibration of scapolite-bearing assemblages, it provides little information on the mechanism by which the granulites studied attained the condition of low a_{H_2O} and high a_{CO_2}. One mechanism invokes pervasive infiltration of CO_2 on a regional scale, and has found wide acceptance as the process by which charnockites developed from gneissic precursors in South India (e.g. Janardhan et al. 1979; Newton et al. 1980b; Friend 1981; Holt and Wightman 1983; Drury et al. 1984; Gopalakrishna et al. 1986). The coincidence of low calculated a_{H_2O}, carbonic fluid inclusions whose densities fall on isochores consistent with peak metamorphic conditions, fluid inclusions whose compositions are distinctly different from hydrous inclusions in amphibolite facies protoliths (Hansen et al. 1984), along with field evidence for pervasive transformation of gneiss to charnockite (Janardhan et al. 1979; Friend 1981; Hansen et al. 1987) are consistent with infiltration of CO_2. Calculated a_{CO_2} for the scapolite-bearing mafic granulites from Doddakanya and Sargur, indicate that the fluid phase was locally CO_2-rich and may have resulted from infiltration, whereas a_{CO_2} for the calc-silicate samples from Satnur indicate either an H_2O-rich fluid or absence of fluid. All these samples lie within the transition zone from amphibolite to granulite facies where the transformation to charnockite is incomplete and where a_{CO_2} may have been locally variable. However, if the infiltration of a_{CO_2} was truly pervasive, all lithologies should show the effects of fluid buffered, fluid/rock interaction. An additional test of the CO_2-flooding hypothesis would be quantitatively to constrain fluid composition using phase equilibria and fluid inclusion analysis in all lithologies within a terrane inferred to have undergone infiltration.

The scapolite-bearing granulites and meta-anorthosite investigated here have bulk compositions, mineral assemblages, and mineral chemistries identical to scapolite-free analogues in other high-grade terranes. Reports of scapolite-bearing mafic granulites and meta-anorthosite are far outnumbered by scapolite-free occurrences. In addition, although scapolite is widely developed in the Furua Complex granulites, Coolen (1980) reports nearly as many scapolite-free samples as scapolite-bearing ones. If scapolite-bearing granulite and meta-anorthosite mineral assemblages generally reflect elevated a_{CO_2}, what does the absence of scapolite from these lithologies imply? The appearance of scapolite in mafic supracrustal granulites may be related to protolith mineralogy (presence of calcite and sulfides) and P-T conditions, where scapolite forms from solid-solid reactions with plagio-

Appendix. Electron Microprobe Analyses

Scapolite analyses

Sample	Calc-silicate		Meta-anorthosite									Mafic Granulite		
	H85A -1e(2)	M86E -1C-2	PS7c	PS85A -2c	PSO85A -8b	PS86E -7e	PS86E -31	S86E -25a	S86E -36b	S86E -41	CCM 0114	S86E -53a	80DMA 614p	85DMP 272-2a
SiO_2	45.77	47.71	46.25	46.54	46.05	46.21	46.87	46.17	46.40	46.07	45.12	46.20	44.69	45.57
Al_2O_3	27.50	26.91	27.63	27.35	27.13	27.51	27.09	27.56	27.22	27.74	26.79	26.05	26.42	26.29
Fe_2O_3	0.14	0.02	0.09	0.07	0.13	0.08	0.08	0.08	0.13	0.10	0.19	0.12	0.09	0.25
CaO	18.65	16.15	18.25	18.15	17.76	17.69	17.58	18.07	17.65	18.33	17.68	16.82	17.33	17.19
Na_2O	3.16	4.32	3.21	3.30	3.38	3.46	3.52	3.42	3.27	3.17	3.27	3.86	3.58	3.75
K_2O	0.14	0.39	0.13	0.11	0.17	0.14	0.11	0.12	0.12	0.10	0.08	0.05	0.08	0.04
Cl	0.06	0.51	0.07	0.07	0.08	0.10	0.14	0.05	0.11	0.01	0.02	0.03	0.07	0.06
SO_3	0.00	0.04	0.03	0.04	0.82	0.10	0.07	0.41	0.59	0.00	4.12	4.14	4.44	4.55
CO_2	4.60	4.19	4.71	4.74	4.21	4.62	4.60	4.51	4.33	4.79	2.39	2.38	2.10	2.09
$-0=Cl$	0.01	0.12	0.02	0.02	0.02	0.02	0.03	0.01	0.02	0.00	0.00	0.01	0.02	0.01
Sum	100.01	100.12	100.35	100.35	99.71	99.89	100.03	100.38	99.80	100.31	99.66	99.64	98.78	99.78
Si	7.05	7.21	7.04	7.09	7.08	7.05	7.14	7.04	7.09	7.02	7.06	7.21	7.07	7.14
Al	4.94	4.79	4.96	4.91	4.92	4.95	4.86	4.96	4.92	4.98	4.94	4.79	4.93	4.86
Fe	0.01	0.00	0.01	0.01	0.02	0.01	0.01	0.01	0.02	0.01	0.02	0.01	0.01	0.03
Ca	3.01	2.61	2.98	2.98	2.93	2.89	2.87	2.95	2.89	2.99	2.96	2.81	2.94	2.69
Na	0.92	1.27	0.95	0.95	1.01	1.02	1.04	1.01	0.97	0.94	0.99	1.17	1.10	1.10
K	0.03	0.08	0.03	0.03	0.03	0.03	0.02	0.02	0.02	0.02	0.02	0.01	0.02	0.01
Cl	0.01	0.13	0.02	0.02	0.02	0.03	0.04	0.01	0.03	0.00	0.00	0.01	0.02	0.02
SO_4	0.00	0.01	0.00	0.01	0.10	0.01	0.01	0.05	0.07	0.00	0.48	0.49	0.53	0.54
CO_3	0.99	0.87	0.98	0.98	0.88	0.96	0.96	0.94	0.90	1.00	0.52	0.51	0.45	0.45

Plagioclase analyses

Sample	H85A -1e(2)	M86E -1C-2	PS7c	PS85A -2c	PSO85A -8b	PS86E -7e	PS86E -31	S86E -25a	S86E -36b	CCM 0114	S86E -53a	80DMA 614p	85DMP 272-2a
SiO_2	55.51	60.79	57.67	54.24	56.19	56.69	57.94	54.92	55.35	52.30	58.14	54.74	57.26
Al_2O_3	28.76	24.64	26.99	29.33	27.60	27.46	26.73	28.58	28.41	30.53	26.30	28.15	26.81
Fe_2O_3	0.10	0.01	0.06	0.05	0.08	0.03	0.04	0.09	0.06	0.08	0.16	0.07	0.04
CaO	10.62	5.84	8.97	11.89	9.56	9.25	8.71	10.60	10.28	12.80	8.06	10.49	8.62
Na_2O	5.42	8.09	6.33	4.90	6.05	6.37	6.55	5.37	5.60	4.09	6.85	5.57	6.72
K_2O	0.22	0.36	0.27	0.15	0.24	0.14	0.13	0.18	0.25	0.20	0.19	0.19	0.12
Sum	100.63	99.73	100.29	100.56	99.72	99.94	100.10	99.74	99.95	100.00	99.70	99.21	99.57
Si	2.49	2.71	2.58	2.44	2.53	2.54	2.59	2.48	2.49	2.37	2.61	2.48	2.57
Al	1.52	1.29	1.42	1.55	1.47	1.45	1.41	1.52	1.51	1.63	1.39	1.51	1.42
Fe	0.00	0.00	0.00	0.00	0.00	0.00	0.00	0.00	0.00	0.00	0.01	0.00	0.00
Ca	0.51	0.28	0.43	0.57	0.46	0.44	0.42	0.51	0.50	0.62	0.39	0.51	0.42
Na	0.47	0.70	0.55	0.43	0.53	0.55	0.57	0.47	0.49	0.36	0.60	0.49	0.59
K	0.01	0.02	0.02	0.01	0.01	0.01	0.01	0.01	0.01	0.01	0.01	0.01	0.01

clase, more than to the composition of the fluid phase or magnitude of fluid activities. If most granulite terranes were pervasively infiltrated by CO_2, or equilibrated in the presence of a pervasive CO_2-bearing fluid phase generated by infiltration or melting reactions that partition H_2O over CO_2, why don't the mafic lithologies in these terranes all contain scapolite?

Source of volatiles in scapolite-bearing rocks

A tacit assumption of the type of calculations presented here is that the calculated a_{CO_2} and a_{H_2O} relate to the near-peak metamorphic equilibration of components involved in scapolite equilibria. This does not imply that the rocks remained free of a fluid phase throughout their entire metamorphic history, or that the low a_{CO_2} attending final equilibration for some samples conflicts with the presence of scapolite in these rocks. The components for stabilization of CO_3/SO_4 scapolite solid solutions may have been introduced at several stages in the formation, alteration and metamorphism of the protoliths for the gneisses and granulites. The Whitestone meta-anorthosite is an example of a scapolite-bearing rock that required fluid infiltration for isotopic enrichment and formation of the metamorphic envelope developed with-

Garnet analyses[1]

Sample	H85A -1e(2)	M86E -1c-2	PS7c	PS85A -2c	PSO85A -8b	PS86B 1-7	PS86E -7e	PS86E -31	S86E -25a	S86E -36b	S86E -41 core	S86E -41 rim	CCM 0114	S86E -53a core	S86E -53a rim	80DMA -614P corona	85DMP -614P porph.	85DMP -272-2a
SiO_2	38.95	39.61	39.06	38.27	38.04	37.15	37.94	38.22	38.67	38.35	38.58	38.60	38.55	39.17	38.93	38.87	38.98	39.59
TiO_2	0.26	0.32	0.00	0.00	0.03	0.04	0.04	0.06	0.05	0.08	0.06	0.03	0.03	0.06	0.02	0.03	0.04	0.01
Al_2O_3	18.73	21.08	21.31	20.93	20.68	20.61	20.11	20.62	20.86	20.71	21.06	20.86	21.20	21.66	21.77	21.19	21.20	21.70
Cr_2O_3	0.05	0.02	0.00	0.00	0.00	0.02	0.00	0.00	0.00	0.02	0.02	0.02	0.02	0.00	0.00	0.03	0.12	0.08
Fe_2O_3	4.23	1.31	0.00	0.88	1.08	0.82	1.66	1.07	1.33	1.33	1.43	1.41	0.72	0.83	0.98	0.82	0.75	0.71
FeO^2	11.34	2.51	24.50	23.80	26.02	31.90	25.95	25.56	24.32	26.44	26.18	25.92	24.75	22.18	23.73	24.38	22.72	22.32
MnO	0.78	0.17	0.76	3.81	0.80	1.51	1.48	1.56	1.34	1.09	0.63	0.71	1.23	0.47	0.99	2.46	3.60	1.03
MgO	0.03	0.06	2.99	1.62	2.49	1.15	1.45	1.20	3.76	3.48	6.63	5.90	5.80	6.78	6.04	5.76	6.33	7.98
CaO	29.19	35.56	12.31	11.98	11.53	7.56	12.33	12.84	11.26	10.30	6.84	7.95	7.77	10.05	9.31	7.20	6.66	7.58
FeO^3	7.54	1.33	24.50	23.02	25.04	31.17	24.45	24.59	23.12	25.24	24.89	24.66	24.01	21.43	22.85	23.65	22.04	21.66
Sum	99.76	99.46	100.93	100.51	99.69	100.03	99.46	100.16	100.39	100.60	100.14	100.14	99.33	100.45	100.89	100.01	99.72	100.34
Si	3.03	3.01	3.03	3.02	3.01	2.99	3.03	3.03	3.02	3.00	2.99	3.00	3.02	3.00	2.99	3.03	3.03	3.02
Ti	0.02	0.02	0.00	0.00	0.00	0.00	0.00	0.00	0.00	0.01	0.00	0.00	0.00	0.00	0.00	0.00	0.00	0.00
Al	1.72	1.89	1.95	1.95	1.93	1.46	1.90	1.93	1.92	1.91	1.93	1.91	1.95	1.95	1.97	1.95	1.95	1.95
Cr	0.00	0.00	0.00	0.00	0.00	0.00	0.00	0.00	0.00	0.00	0.00	0.00	0.00	0.00	0.00	0.00	0.01	0.01
Fe^{3+}	0.25	0.08	0.00	0.05	0.07	0.05	0.10	0.06	0.08	0.08	0.08	0.08	0.05	0.05	0.06	0.05	0.04	0.04
Fe^{2+}	0.49	0.09	1.59	1.52	1.66	2.10	1.64	1.63	1.51	1.66	1.62	1.61	1.57	1.37	1.47	1.54	1.44	1.39
Mn	0.05	0.00	0.05	0.26	0.05	0.10	0.10	0.11	0.09	0.07	0.04	0.05	0.08	0.03	0.06	0.16	0.24	0.07
Mg	0.00	0.01	0.35	0.19	0.29	0.14	0.17	0.14	0.44	0.41	0.77	0.68	0.68	0.77	0.69	0.67	0.74	0.91
Ca	2.44	2.90	1.02	1.01	0.98	0.65	1.06	1.09	0.94	0.86	0.57	0.66	0.65	0.82	0.77	0.60	0.56	0.62

[1] normalized to 8 cations; Fe^{3+} = greater of 8-2Si-2Ti-Al-Cr or 2-Al. [2] Total Fe calculated as FeO from microprobe analysis
[3] wt% FeO recalculated from estimate of Fe^{3+} and used to calculate oxide sum

in the margin of the pluton, and for which there is an obvious local source of CO_2-bearing fluid. However, the mechanism for introducing volatile components into protoliths for scapolite-bearing granulites and xenoliths is less apparent. In many cases the protoliths for mafic granulites are components of supracrustal sequences and may be mafic volcanics (e.g. Furua Complex, Coolen 1980). Sulfur derived from oxidation of sulfides may be incorporated as sulfate in scapolite during metamorphism. Textural evidence for such a process is sulfate-bearing scapolite mantling sulfides in the Whitestone meta-anorthosite (Moecher, unpublished data). Sulfate may be dissolved in a mafic melt, or sulfur may be introduced as an oxidized species prior to metamorphism. Possible sources of carbon include (1) the presence of dissolved magmatic carbonate in the volcanic protoliths, or, in the case of the granulite facies core of the WSA and in the Bergen Arcs meta-anorthosites, in anorthositic magma; (2) late carbonate introduced during alteration of mafic protoliths; or (3) infiltration of CO_2.

Although granulites from regional terranes include supracrustal lithologies, granulite xenoliths may not have had a previous upper crustal history. The majority of the xenoliths have basaltic bulk compositions, and are interpreted as the recrystallized equivalents of, or cumulates derived from, mafic magmas emplaced at the base of the crust or in the upper mantle (Lovering and White 1969; Wilkinson 1974; Edwards et al. 1979; Rudnick and Taylor 1987; Thomas and Nixon 1987; Stolz and Davies 1989). These melts have subsequently experienced metamorphic recrystallization to scapolite-bearing, garnet-plagioclase clinopyroxenite or granulite assemblages. Recrystallization pressures of the xenoliths are distinctly higher than most exposed granulite terranes, approaching 15 kbar (Griffin et al. 1979; Jones et al. 1983; Bohlen and Mezger 1989; this study, Table 1). If they crystallized directly at these depths without prior subaerial exposure, the subsequent formation of scapolite requires a mechanism for incorporating CO_2 and SO_2 into these rocks. The solubility of CO_2 in tholeiitic basalt ranges from 1.7 to 3.3 wt. percent at 15 to 30 kbar and 1450 to 1650° C (Mysen et al. 1975). Spera and Bergman (1980) have modeled the solubility of CO_2 in tholeiite to lower pressures. The solubility of CO_2 at liquidus temperatures for lower pressures (approx. 1200° C at 10–15 kbar) is much less, on the order of 0.1 wt. percent. However, this is an adequate quantity to account for the small modal abundances of carbonate/sulfate scapolite found in many xenoliths. Because CO_2 and sulfur dissolve as CO_3^{-2} and SO_3^{-2} (Holloway 1981), these components may be incorporated into scapolite crystallizing from a melt (e.g. Goff et al. 1982). Scapolite xenoliths may be the recrystallized equivalents of CO_2 and sulfide-bearing melts emplaced at the base of the crust. Carbon isotope studies are underway to evaluate the source of carbon in scapolite from granulites and lower crustal xenoliths.

Acknowledgments. This paper comprises a chapter of the dissertation research of DPM at the University of Michigan. Work was supported by NSF Grants EAR-84-08169 and EAR-88-05083, and

Pyroxene Analyses[1]

	Clinopyroxene												Orthopyroxene	
Sample	H85A -1e(2)	M86E -1c-2	PS7c	PS86B1 -7	S86E 25a	S86E -36b	S86E -41 core	S86E -41 rim	S86E -53a	80DMA -614p core	80DMA -614p rim	85DMP -272-2a	80DMA -614p	85DMP -272-2a
SiO_2	48.15	53.09	50.96	49.42	49.51	49.02	49.98	50.70	51.53	50.90	51.36	50.52	51.95	53.04
TiO_2	0.29	0.00	0.14	0.01	0.61	0.41	0.43	0.35	0.33	0.33	0.33	0.46	0.03	0.03
Al_2O_3	2.18	0.99	2.27	1.18	5.29	4.40	4.04	3.55	3.41	3.75	3.68	4.79	2.04	2.00
Cr_2O_3	0.00	0.01	0.00	0.01	0.03	0.02	0.00	0.00	0.00	0.04	0.05	0.06	0.02	0.04
Fe_2O_3	1.08	0.00	4.67	2.67	1.76	3.39	2.85	2.22	1.13	1.51	2.12	2.96	2.12	0.10
FeO[2]	23.72	9.82	11.76	20.25	11.65	13.09	9.83	8.71	8.16	9.45	8.40	8.33	23.80	21.39
MnO	0.75	0.08	0.11	0.23	0.17	0.08	0.07	0.04	0.10	0.48	0.20	0.13	1.44	0.30
MgO	2.94	11.43	11.36	5.90	10.13	9.51	11.88	12.16	12.80	11.89	12.74	12.51	20.23	23.19
CaO	21.14	24.13	23.90	20.65	21.14	21.57	21.79	22.65	22.28	21.45	22.06	21.66	0.61	0.33
Na_2O	0.63	0.31	0.54	0.87	0.94	0.92	0.80	0.75	0.71	0.84	0.87	1.07	0.03	0.01
FeO[3]	22.75	9.82	7.56	17.85	10.07	10.04	7.26	6.72	7.15	8.09	6.49	5.67	21.89	21.30
Sum	99.91	99.86	101.51	98.79	99.65	99.36	99.10	99.14	99.44	99.28	99.90	99.83	100.36	100.34
Si	1.95	2.00	1.90	1.97	1.87	1.87	1.89	1.91	1.93	1.92	1.91	1.88	1.93	1.95
Ti	0.01	0.00	0.00	0.00	0.02	0.01	0.01	0.01	0.01	0.01	0.01	0.01	0.00	0.00
Al^{iv}	0.05	0.00	0.10	0.03	0.13	0.13	0.11	0.09	0.07	0.08	0.09	0.12	0.07	0.05
Al^{vi}	0.05	0.04	0.00	0.03	0.11	0.07	0.07	0.07	0.08	0.09	0.07	0.09	0.02	0.04
Cr	0.00	0.00	0.00	0.00	0.00	0.00	0.00	0.00	0.00	0.00	0.00	0.00	0.00	0.00
Fe^{3+}	0.03	0.00	0.13	0.08	0.05	0.10	0.08	0.06	0.03	0.09	0.06	0.08	0.06	0.00
Fe^{2+}	0.77	0.31	0.24	0.59	0.32	0.32	0.23	0.21	0.22	0.26	0.20	0.18	0.68	0.66
Mn	0.03	0.00	0.00	0.01	0.01	0.00	0.00	0.00	0.00	0.02	0.01	0.00	0.05	0.01
Mg	0.15	0.64	0.63	0.35	0.57	0.54	0.67	0.68	0.71	0.67	0.71	0.69	1.17	1.27
Ca	0.92	0.98	0.96	0.88	0.86	0.88	0.88	0.01	0.89	0.87	0.88	0.86	0.03	0.01
Na	0.05	0.02	0.04	0.08	0.07	0.07	0.06	0.06	0.05	0.06	0.06	0.08	0.00	0.00

[1] normalized to 4 cations; Fe^{3+} = greater of 4-2Si-2Ti-Al-Cr or 2-Al

[2] Total Fe calculated as FeO from microprobe analysis

[3] Wt% FeO recalculated from estimate of Fe^{3+}

Epidote Analyses

Sample	PS85A -2c	PS86E -7e	PS86E -31	S86E -25a
SiO_2	38.71	37.82	38.95	38.53
TiO_2	na	0.15	na	0.15
Al_2O_3	26.21	25.90	25.73	27.22
Fe_2O_3	9.93	10.22	10.96	8.57
Mn_2O_3	0.02	0.06	0.11	0.04
CaO	23.74	23.43	23.27	23.25
H_2O	1.92	1.90	1.92	1.91
Sum	100.53	99.48	100.94	99.67
Si	3.02	2.99	3.04	3.02
Ti	–	0.01	–	0.01
Al	2.41	2.41	2.37	2.51
Fe^{3+}	0.58	0.61	0.64	0.51
Mn^{3+}	0.00	0.00	0.01	0.00
Ca	1.98	1.98	1.94	1.95
OH[1]	1.00	1.00	1.00	1.00

[1] OH assumed to be 1.00

grants-in-aid from the Turner Fund of the University of Michigan, the Geological Society of America, and Sigma Xi. The electron microprobe used in this study was obtained with NSF grant EAR-82-12764 and matching funds from the University of Michigan.

The critical comments of R.J. Arculus, D.R. Peacor, Z.D. Sharp, and J.W. Valley are greatly appreciated. The reviews of J.Y. Bradshaw, J.M. Ferry, and C.I. Mora were particularly helpful in revising the manuscript. H. Austrheim, A. Davidson, T.C. Devaraju, Chris Marmont, C. Srikantappa, and A.J. Stolz generously provided samples that allowed expansion of the scope of this study, and J.Y. Bradshaw provided unpublished microprobe analyses. Discussions with R.C. Newton, H.G. Huckenholz, and W.M. Lamb were most helpful.

References

Anovitz LM, Essene EJ (1987) Compatibility of geobarometers in the system $CaO-FeO-Al_2O_3-SiO_2-TiO_2$: implications for garnet mixing models. J Geol 95:633–645

Anovitz LM, Essene EJ (1990) Thermobarometry and pressure-temperature paths in the Grenville Province, Ontario. J Petrol 31:197–241

Austrheim H, Griffin WL (1985) Shear deformation and eclogite formation within granulite-facies anorthosites of the Bergen Arcs, western Norway. Chem Geol 50:267–281

Bhattacharya A, Sen SK (1986) Granulite metamorphism, fluid buffering, and dehydration melting in the Madras charnockites and metapelites. J Petrol 27:1119–1141

Bohlen SR, Mezger K (1989) Origin of granulite terranes and the formation of the lowermost continental crust. Science 244:326–329

Bohlen SR, Peacor DR, Essene EJ (1980) Crystal chemistry of a metamorphic biotite and its significance in water barometry. Am Mineral 65:55–62

Bohlen SR, Boettcher AL, Wall VJ, Clemens JD (1983a) Stability of phlogopite-quartz and sanidine-quartz: a model for melting in the lower crust. Contrib Mineral Petrol 83:270–277

Bohlen SR, Wall VJ, Boettcher AL (1983b) Geobarometry in granulites. In: Saxena S (ed) Kinetics and Equilibrium in Mineral Reactions. Springer-Verlag, Berlin, pp 141–171

Boivin P, Camus G (1981) Igneous scapolite-bearing associations in the Chaine des Puys, Massif Central (France) and Atakor (Hoggar, Algeria). Contrib Mineral Petrol 77:365–375

Bradshaw JY (1985) Geology of the northern Franklin Mountains, northern Fiordland, New Zealand, with emphasis on the origin and evolution of Fiordland granulites. PhD thesis, University of Otago

Bradshaw JY (1989a) Early Cretaceous vein-related garnet granulite in Fiordland southwest New Zealand: a case for infiltration of mantle-derived CO_2-rich fluids. J Geol 97:697–717

Bradshaw JY (1989b) Origin and metamorphic history of an Early Cretaceous polybaric granulite terrain, Fiordland, southwest New Zealand. Contrib Mineral Petrol 103:346–360

Bright EG (1987) Precambrian geology of the Whitestone Lake Area, District of Parry Sound. Ont Geol Surv Map P3095

Brown PE, Lamb WM (1989) P-V-T properties of fluids in the system $H_2O \pm CO_2 \pm NaCl$: New graphical presentations and implications for fluid inclusion studies. Geochim Cosmochim Acta 53:1209–1221

Carswell DA, Griffin WL (1981) Calculation of equilibration conditions for garnet granulite and garnet websterite nodules in African kimberlite pipes. Tschermaks Mineral Petrogr Mitt 28:229–244

Clemens JP, Circone S, Navrotsky A, McMillan PF, Smith BK, Wall VJ (1987) Phlogopite: High temperature solution calorimetry, thermodynamic properties, $Al-Si$ and stacking disorder, and phase equilibria. Geochim Cosmochim Acta 51:2569–2578

Coolen JJMMM (1980) Chemical Petrology of the Furua Granulite Complex, southern Tanzania. GUA Papers of Geology Ser 1, No 13-1980

Coolen JJMMM (1982) Carbonic fluid inclusions in granulites from the Furua Complex, Tanzania – a comparison of geobarometric methods based on fluid density and mineral chemistry. Chem Geol 37:59–77

Davidson A (1984) Tectonic boundaries within the Grenville Province of the Canadian Shield. Geodynam 1:433–444

Davidson A (1986) New interpretations in the southwestern Grenville Procince. In: Moore JM, Davidson A, Baer AJ (eds) The Grenville Province, Geol Assoc Can Spec Pap 31:61–74

Devaraju TC, Coolen JJMMM (1983) Mineral chemistry and P-T conditions of formation of a basic scapolite-garnet-pyroxene granulite from Doddakanya, Mysore District. J Geol Soc India 24:404–411

Devaraju TC, Gowd Reddy K (1976) Coexisting orthopyroxene and scapolite in certain basic granulites from Doddakanya, Mysore District. Indian Mineral 17:5–11

Devaraju TC, Sadashivaiah MS (1964) Calc-silicate xenoliths in the charnockites of Satnur, Mysore [Karnataka] State. Indian Mineral 5:105–116

Drury SA, Harris NBW, Holt RW, Reeves-Smith GJ, Wightman RT (1984) precambrian tectonics and crustal evolution in South India. J Geol 92:3–20

Edwards AC, Lovering JF, Ferguson J (1979) High pressure basic inclusions from the Kayrunnera kimberlitic diatreme in New South Wales, Australia. Contrib Mineral Petrol 69:185–192

Elkins LT, Grove TL (1990) Ternary feldspar experiments and thermodynamic models. Am Mineral 75:544–559

Ellis DE (1978) Stability and phase equilibria of chloride and carbonate scapolite at 750° C and 4000 bars. Geochim Cosmochim Acta 42:1271–1281

Ellis DJ, Green DH (1979) An experimental study of the effect of Ca upon garnet-clinopyroxene $Fe-Mg$ exchange equilibria. Contrib Mineral Petrol 71:13–22

Eskola P (1939) Die metamorphen Gesteine, "Die Entstehung der Gesteine". In: Barth TFW, Correns TW, Eskola P (eds) Springer, Berlin, pp 263–407

Essene EJ (1989) The current status of thermobarometry in metamorphic rocks. In: Daly S, Cliff R, Yardley B (eds) The Evolution of Metamorphic Belts. Spec Pub Geol Soc London Vol. 42, pp 1–44

Evans BW, Shaw DM, Houghton DR (1969) Scapolite Stoichiometry. Contrib Mineral Petrol 24:293–305

French BM (1966) Some geological implications of equilibrium between graphite and a $C-H-O$ gas phase at high temperatures and pressures. Rev. Geophys 4:223–253

Friend CRL (1981) Charnockite and granite formation and influx of CO_2 at Kabbaldurga. Nature 294:550–552

Frost BR, Frost CD (1987) CO_2, melts and granulite facies metamorphism. Nature 327:503–506

Ganguly J, Saxena SK (1987) Mixtures and Mineral Reactions. Springer-Verlag, Berlin 291 p.

Glassley WE (1983) Deep crustal carbonates as CO_2 fluid sources-evidence from metasomatic reaction zones. Contrib Mineral Petrol 84:15–24

Goff F, Arney BH, Eddy AC (1982) Scapolite phenocrysts in a latite dome, northwest Arizona, U.S.A. Earth Planet Sci Lett 60:86–92

Goldsmith JR, Newton RC (1977) Scapolite-plagioclase stability relations at high pressures and temperatures in the system $NaAlSi_3O_8-CaAl_2Si_2O_8-CaCO_3-CaSO_4$. Am Mineral 62:1063–1081

Gopalakrishna D, Hansen EC, Janardhan AS, Newton RC (1986) The southern high-grade margin of the Dharwar Craton. J Geol 94:247–260

Griffin WL, O'Reilly SY (1987) The composition of the lower crust and the nature of the continental Moho-xenolith evidence. In: Nixon PH (ed) Mantle Xenoliths, John Wiley and Sons, Chichester, New York, pp 413–430

Griffin WL, Carswell DA, Nixon PH (1979) Lower-crustal granulites and eclogites from Lesotho, southern Africa. In: Boyd FR, Meyer HOA (eds) Xenoliths and Megacrysts, Proceedings of the 2nd Int Kimberlite Conference. Am Geophys Union, Washington, pp 59–86

Hansen EC, Newton RC, Janardhan AS (1984) Fluid inclusions in rocks from the amphibolite-facies gneiss to charnockite progression in southern Karnataka, India: direct evidence concerning the fluids of granulite metamorphism. J Metamorph Geol 2:249–264

Hansen EC, Janardhan AS, Newton RC, Prame WKBN, Ravindra Kumar GR (1987) Arrested charnockite formation in southern India and Sri Lanka. Contrib Mineral Petrol 96:225–244

Hewitt DA, Wones DR (1975) Physical properties of some synthetic $Fe-Mg-Al$ trioctahedral biotites. Am Mineral 58:889–900

Hietanen A (1967) Scapolite in the Belt Series in the St. Joe-Clearwater region, Idaho. Geol Soc Am Spec Pap 86

Holloway JR (1977) Fugacity and activity of molecular species in supercritical fluids. In: Fraser DG (ed) Thermodynamics in Geology, Reidel, Dodrecht-Holland, pp 161–181

Holloway JR (1981) Volatile interactions in magmas. In: Newton RC, Navrotsky A, Wood BJ (eds) Thermodynamics of Minerals and Melts. Springer, Berlin Heidelberg New York, pp 273–293

Holt RW, Wightman RT (1983) The role of fluids in the development of a granulite facies transition zone in S India. J Geol Soc London 140:651–656

Huckenholz HG, Seiberl W (1989) Occurrence of carbonate scapolites and their bearing on geothermometry of rock of (high-temperature) granulite facies (abstract). 28th Int Geol Cong:2–79

Janardhan AS, Gopalakrishna D (1983) Pressure-temperature estimates of the basic granulites and conditions of metamorphism in Sargur terrain, southern Karnataka and adjoining areas. J Geol Soc India 24:219–228

Janardhan AS, Srikantappa C (1975) Geology of the northern parts of the Sargur schist belt between Mavinahalli and Dodkanya, Mysore District, Karnataka. Indian Mineral 16:66–75

Janardhan AS, Newton RC, Smith JV (1979) Ancient crustal metamorphism at low p_{H_2O}: charnockite formation at Kabbaldurga, south India. Nature 278:511–514

Jin S, Li D, Li X, Liu F (1988) Metamorphic characteristics of granulite facies rocks in the Laixi-Pingdu area in eastern Shandong Province. Acta Geol Sinica 1:59–74

Johnson CA, Bohlen SR, Essene EJ (1983) An evaluation of garnet-clinopyroxene geothermometry in granulites. Contrib Mineral Petrol 84:191–198

Jones AP, Smith JV, Dawson JB, Hansen EC (1983) Metamorphism, partial melting, and K-metasomatism of garnet-scapolite-kyanite granulite xenoliths from Lashaine, Tanzania. J Geol 91:143–165

Kay RW, Kay SM (1981) The nature of the lower continental crust: inferences from geophysics, surface geology, and crustal xenoliths. Rev Geophys Space Phys 19:271–297

Kerrick DM, Jacobs GK (1981) A modified Redlich-Kwong equation for H_2O, CO_2, and H_2O-CO_2 mixtures at elevated pressures and temperatures. Am J Sci 281:735–767

Kwak TAP (1977) Scapolite compositional change in a metamorphic gradient and its bearing on the identification of meta-evaporite sequences. Geol Mag 114:343–354

Lamb WM, Valley JW (1985) $C-O-H$ fluid calculations and granulite genesis. In: Tobi AC, Touret JLR (eds) The Deep Proterozoic Crust in the North Atlantic Provinces. Reidel, Dordrecht, Boston, pp 119–131

Lamb WM, Valley JW (1988) Calculation of water activities in the Adirondack Mountains, NY. Contrib Mineral Petrol 100:349–360

Lamb WM, Valley JW, Brown PE (1987) Post-metamorphic CO_2-rich fluid inclusions in granulites. Contrib Mineral Petrol 96:485–495

Lovering JF, White AJR (1964) The significance of primary scapolite in granulitic inclusions from deep-seated pipes. J Petrol 5:195–218

Lovering JF, White AJR (1969) Granulitic and eclogitic inclusions from basic pipes at Delegate, Australia. Contrib Mineral Petrol 21:9–52

Mason IM (1969) Petrology of the Whitestone Anorthosite. PhD Thesis, McMaster Univ

Mezger K, Okrusch M (1985) Metamorphism of the variegated sequence at Kallithea, Samos, Greece. Tschermaks Mineral Petrogr Mitt 34:67–82

Moecher DP (1988) Scapolite phase equilibria and carbon isotope variations in high-grade rocks: tests of the CO_2-flooding hypothesis of granulite genesis. PhD Thesis, Univ Michigan

Moecher DP, Essene EJ (1990a) Scapolite phase equilibria: additional constraints on the role of CO_2 in granulite genesis. In: Vielzeuf D, Vidal P (eds) Granulites and Crustal Evolution, Kluwer, Dordrecht, Boston, pp 385–396

Moecher DP, Essene EJ (1990b) Calculation of CO_2 activities in scapolite-bearing rocks: constraints on the role of CO_2 in high-grade metamorphism. Geol Soc Am Abs Progs 22:70

Moecher DP, Essene EJ (1990c) Phase equilibria for calcic scapolite, and implications of variable $Al-Si$ disorder for P-T, T-X_{CO_2}, and a-X relations. J Petrol 31:997–1024

Moecher DP, Essene EJ, Anovitz LM (1988a) Calculation and application of clinopyroxene-garnet-plagioclase-quartz geobarometers. Contrib Mineral Petrol 100:92–106

Moecher DP, Essene EJ, Valley JW (1988b) Stable isotopic and petrologic constraints on interactions between meta-anorthosite and marble. Geol Soc Amer Abs Progs 20:A46

Mora CI, Valley JW (1989) Halogen-rich scapolite and biotite: implications for metamorphic fluid-rock interaction. Am Mineral 74:721–737

Mysen BO, Arculus RJ, Eggler DH (1975) Solubility of carbon dioxide in melts of andesite, tholeiite, and olivine nephelinite composition to 30 kbar presure. Contrib Mineral Petrol 53:227–239

Nadeau L (1983) Deformation of leucogabbroic rocks at Parry Sound, Ontario. MSc Thesis, Carleton Univ

Newton RC (1986) Fluids of granulite facies metamorphism. In: Walther JV, Wood BJ (eds) Fluid-rock interactions during metamorphism (Advances in physical geochemistry, Vol. 5). Springer, New York, pp 36–59

Newton RC, Perkins D (1982) Thermodynamic calibration of geobarometers based on the assemblages garnet – plagioclase – orthopyroxene – clinopyroxene – quartz. Am Mineral 67:203–222

Newton RC, Charlu TV, Kleppa OJ (1980a) Thermochemistry of the high structural state plagioclases. Geochim Cosmochim Acta 44:933–941

Newton RC, Smith JV, Windley BF (1980b) Carbonic metamorphism, granulites and crustal growth. Nature 288:45–49

Okrusch M, Schröder B, Schnütgen A (1979) Granulite-facies metabasite ejecta in the Laacher See area, Eifel, West Germany. Lithos 12:251–270

Oterdoom H, Gunter WD (1983) Activity models for plagioclase and CO_3-scapolites: an analysis of field and laboratory data. Am J Sci 283-A:255–282

Oterdoom H, Wenk H-R (1983) Ordering and composition of scapolite: field observations and structural interpretations. Contrib Mineral Petrol 83:330–341

Pattison D, Newton RC (1989) Reversed experimental calibration of the garnet-clinopyroxene $Fe-Mg$ exchange thermometer. Contrib Mineral Petrol 101:87–103

Percival JA (1983) High-grade metamorphism in the Chapleau-Foleyet area, Ontario. Am Mineral 53:227–239

Perkins D, Essene EJ, Wall VJ (1987) THERMO: A computer program for calculation of mixed-volatile equilibria. Am Mineral 72:446–447

Phillips GN (1980) Water activity changes across an amphibolite-granulite facies transition, Broken Hill, Australia. Contrib Mineral Petrol 75:377–386

Powell R (1974) A comparison of some mixing models for some silicate crystalline solutions. Contrib Miner Petrol 46:265–274

Robie RA, Hemingway BS (1984) Heat capacities and entropies of phlogopite ($KMg_3[AlSi_3O_{10}](OH)_2$) and paragonite ($NaAl_2[AlSi_3O_{10}](OH)_2$) between 5 and 900 K and estimates of the enthalpies and Gibbs free energies of formation. Am Mineral 69:858–868

Robie RA, Hemingway BS, Fisher JR (1978) Thermodynamic properties of minerals and related substances at 298.15 K and 1 bar (10^5 pascals) pressure and at higher temperatures. US Geol Surv Bull 1452, reprinted with corrections, 1979

Rollinson HR (1980) Mineral reactions in a granulite facies calc-silicate rock from Scourie. Scott J Geol 16:153–164

Rudnick RL, Taylor SR (1987) The composition and petrogenesis of the lower crust: a xenolith study. J Geophys Res 92:13981–14005

Santosh M (1986) Carbonic metamorphism of charnockites in the southwestern Indian Shield: a fluid inclusion study. Lithos 19:1–10

Schenk V (1984) Petrology of felsic granulites, metapelites, metabasics, ultramafics, and metacarbonates from Calabria (Italy): prograde metamorphism, uplift and cooling of a former lower crust. J Petrol 25:255–298

Schreurs J (1984) The amphibolite-granulite facies transition in West Uusimaa, S.W. Finland. A fluid inclusion study. J Metamorph Geol 2:327–341

Spera FJ, Bergman SC (1980) Carbon dioxide in igneous petrogenesis: I Aspects of the dissolution of CO_2 in silicate liquids. Contrib Mineral Petrol 74:55–66

Srikantappa C, Raith M, Ackermand D (1985) High-grade regional metamorphism of ultramafic and mafic rocks from the Archaean Sargur Terrane, Karnataka, South India. Precambrian Res 30:189–219

Stolz AJ (1987) Fluid activity in the lower crust and upper mantle: mineralogical evidence bearing on the origin of amphibole and scapolite in ultramafic and mafic granulite xenoliths. Mineral Mag 51:719–732

Stolz AJ, Davies GR (1989) Metasomatized lower crustal and upper mantle xenoliths from north Queensland: Chemical and isotopic evidence bearing on the composition and source of the fluid phase. Geochim Cosmochim Acta 53:649–660

Thomas CW, Nixon PH (1987) Lower crustal granulite xenoliths in carbonatite volcanoes of the Western Rift of East Africa. Mineral Mag 51:621–633

Thompson AB (1983) Fluid-absent metamorphism. J Geol Soc London 140:533–547

Thompson DL (1983) The nature of anorthosite-country rock interaction during granulite facies metamorphism. MSc thesis, McMaster University, Hamilton, Ontario, 311 pp

Turner FJ (1981) Metamorphic Petrology, 2nd Edition. McGraw-Hill, New York

Valley JW, McLelland J, Essene EJ, Lamb W (1983) Metamorphic fluids in the deep crust: evidence from the Adirondacks. Nature 301:226–228

van Breemen O, Davidson A, Loveridge WD, Sullivan RW (1986) U-Pb geochronology of Grenville tectonites, granulites and igneous precursors, Parry Sound, Ontario. In: Moore JM, Davidson A, Baer AJ (eds) The Grenville Province. Geol Assoc Can Spec Pap 31:191–207

Vanko DA, Bishop FC (1982) Occurrence and origin of marialitic scapolite in the Humboldt Lopolith, N.W. Nevada. Contrib Mineral Petrol 81:277–289

Viswanatha MN, Ramakrishnan M (1981) Sargur and allied belts. In: Swami Nath J, Ramakrishnan M (eds) Early Precmbrian supracrustals of southern Karnataka. Geol Surv India Mem 112:41–59

Wells PRA (1979) Chemical and thermal evolution of Archaean sialic crust, southern West Greenland. J Petrol 20:187–226

Wilkinson JFG (1974) Garnet clinopyroxenite inclusions from diatremes in the Gloucester area, New South Wales, Australia. Contrib Mineral Petrol 46:275–299

Winkler HGF (1979) Petrogenesis of metamorphic rocks, 5th Edition. Springer, Berlin

Editorial responsibility: J. Ferry